

DENSITY FUNCTIONAL THEORY FOR
INHOMOGENEOUS FLUIDS I:
Simple Fluids in Equilibrium

Lectures at 3rd Warsaw School of Statistical Physics
Kazimierz Dolny, 27 June-3 July 2009

R. Evans
H. H. Wills Physics Laboratory,
University of Bristol, Bristol, BS8 1TL, UK

Contents

1	Preamble	2
2	Basic Statistical Mechanics of Classical Fluids	4
2.1	Classical fluids	5
2.2	Effective Hamiltonians and Model Fluids	6
2.3	Partition functions and Thermodynamics	6
2.4	Structure and Thermodynamic Properties of Bulk Liquids	8
3	Introducing Equilibrium Classical DFT	10
4	Summary of DFT Formalism for a Simple Fluid	12
4.1	Generating Functionals and Hierarchies of Correlation Functions	12
4.2	The Free-Energy via Integration	16
4.3	Hard Rods in One Dimension: An Exactly Solvable Model	17
5	Approximate Free Energy Functionals	20
5.1	The Strategy and its Shortcomings	20
5.2	Two Generic Examples	21
5.2.1	Square-Gradient Approximation	21
5.2.2	Density Expansions	23
5.3	Approximations for Specific Model Fluids	27
5.3.1	Hard-Sphere Fluids	27
5.3.2	The Lennard-Jones (LJ) Type Fluid	38
5.3.3	Soft Core Model Fluids: the RPA Functional	40
6	Concluding Remarks	45
	References	47

Chapter 1

Preamble

These lecture notes are intended as an introduction to the equilibrium classical density functional theory (DFT) of simple fluids. The subject has grown enormously since its development and first applications more than thirty years ago and DFT is now regarded as a standard tool or technique in the statistical physics of liquids. The 3rd edition of a classic textbook on the theory of liquids [1] devotes whole sections to DFT and there are treatments in more general textbooks on statistical physics, e.g. [2]. In these lectures the aim is not to present a comprehensive review of the field, which is very large, rather it is to give an overview of the DFT formalism and to describe some recent developments in constructing approximate free energy functionals that have been used to determine the thermodynamic properties, phase behaviour and microscopic structure of inhomogeneous fluids.

An inhomogeneous fluid is one for which $\rho(\mathbf{r})$, the average one-body particle (or atomic) density, is spatially varying. This is in contrast with the case of a uniform or bulk fluid where the average number density ρ is constant. Inhomogeneous situations arise

- i) at *interfaces* between liquid-gas, liquid-liquid (in fluid mixtures), crystal-liquid and crystal-gas phases at bulk coexistence. Translational invariance of the fluid is broken spontaneously and the average density varies through the interfacial region that separates the two phases. This density variation at the microscopic level gives rise to the surface tension of the macroscopic interface.
- ii) in the *adsorption* of liquids or gases at solid substrates or walls. The latter exert an (external) potential $V(\mathbf{r})$ on the particles or atoms of the fluid adsorbate that can produce highly structured density distributions close to the walls and may also lead to macroscopically thick (wetting) films in the limit where the adsorbate is at bulk coexistence. A plethora of surface phase transitions can occur including critical and complete wetting, pre-wetting and layering. These correspond to non-analyticities of the surface excess free energy which is defined by subtracting the bulk free energy from the total at the given thermodynamic state point. Recall that bulk phase boundaries are determined by non-analyticities of the bulk free

energy density.

- iii) for fluids in *confining geometries*, e.g. fluids confined in microchannels, in porous solids or in wedges. The finite size of the pore and the wall-fluid interactions give rise to profound effects on the structure of the fluid and on the phase behaviour. Capillary condensation and capillary filling are examples of phase transitions arising from confinement. In experiments that exploit the surface force apparatus (SFA) a fluid is confined (effectively) between two plates whereas in the atomic force microscope (AFM) the confinement is between the tip and a substrate.
- iv) sedimentation of colloidal fluids in a gravitational field.

There are, of course, many other physical situations and phenomena that require an understanding of the properties of inhomogeneous fluids from a microscopic basis, i.e. a description that starts with atoms or molecules (or ‘particles’) and the interactions between these basic building blocks of matter. Equilibrium DFT is a technique that provides a general framework for calculating density profiles, correlation functions, excess free energies and phase behaviour for model fluids defined by a given effective Hamiltonian and treated by classical statistical mechanics. Although the DFT formalism (Chapter 4) is quite general, and some generic approximations are quite versatile, applications often require the construction of an approximate intrinsic free-energy functional specifically designed for the model fluid under consideration. Much recent research has focused on finding functionals that can treat accurately and reliably: a) hard-sphere fluids and their mixtures, both additive and non-additive. These are important as reference systems for atomic fluids and as models for colloidal suspensions. b) Lennard-Jones type models, appropriate for rare gas fluids. c) Repulsive soft core models, used to describe the effective interactions between the centres of mass of polymer coils. These are so-called ‘blob’ models that have integrated out monomer degrees of freedom. We describe this work in Chapter 5. Chapter 2 is aimed at those readers who require a brief reminder of the basic equilibrium statistical mechanics of classical fluids, i.e. partition functions and correlation functions in bulk liquids. Chapter 3 introduces the basic idea of classical DFT.

We focus on *simple fluids* and their mixtures where the interparticle or interatomic potential function is pairwise additive and the pair potential depends only on the distance between the centres of the particles. It is for these model systems that DFT approximations are well-developed. In the second DFT course at this school Hartmut Löwen will describe DFT treatments of bulk freezing. A crystal can be regarded as a particular class of density inhomogeneity where $\rho(\mathbf{r})$ is periodic and thus, in principle, DFT should account for the freezing transition. Löwen’s lectures will also describe DFT treatments of rod-like particles that exhibit orientational degrees of freedom and liquid crystalline ordering. He will describe developments in dynamical density functional theory (DDFT) now widely used in treating nonequilibrium problems for colloidal suspensions where the underlying dynamics is Brownian.

Chapter 2

Basic Statistical Mechanics of Classical Fluids

In this chapter we provide a brief reminder of the basic equilibrium statistical mechanics of classical fluids. The emphasis is on the properties of uniform (bulk) fluids for which the average number density ρ is a constant and a thermodynamic state point is specified by ρ and temperature T . For simplicity we consider one component fluids.

We include this chapter as introductory material for those readers who have not taken a course on simple fluids. Details of derivations are omitted; a thorough account is given in the textbook by Hansen and McDonald [1].

The *general strategy* for understanding the equilibrium properties of the liquid state of matter follows that of other parts of statistical physics. Namely one defines ‘particles’ and the interactions between these to construct an effective Hamiltonian, i.e. the theorist constructs a model fluid. Liquids are usually tackled within the framework of classical statistical mechanics since the mass of the particle is large and T is high. Thermodynamic quantities such as the internal energy, pressure, compressibility and heat capacity are obtained as derivatives of the classical partition function. Phase transitions between liquids and gases and between liquids and solids correspond to non-analyticities in the appropriate thermodynamic potentials calculated in the thermodynamic limit where the number of particles $N \rightarrow \infty$, and the volume of the system $V \rightarrow \infty$ in such a way that the average number density $\rho = N/V$ is constant. The equilibrium structure of a fluid is described in terms of hierarchies of distribution or correlation functions. Formally these correspond to functional derivatives of the partition function w.r.t. an external potential and will be described in Chapter 4. The two-body correlation function of a uniform fluid can be obtained from experiment—see Section 2.4. Many theorists opt to study very simple models and focus on comparing the results of their approximate theory with those from computer simulation of the same model. Other researchers prefer to introduce more realistic models that capture more features of the real, experimental systems.

Since one normally adopts a classical approach from the outset computer simulations are quite straightforward, once the model fluid is specified. The two main techniques

are Monte Carlo and Molecular Dynamics and the books by Allen and Tildesley [3], and Frenkel and Smit [4] provide excellent introductions to this subject. Figure 2.1 outlines the overall strategy.

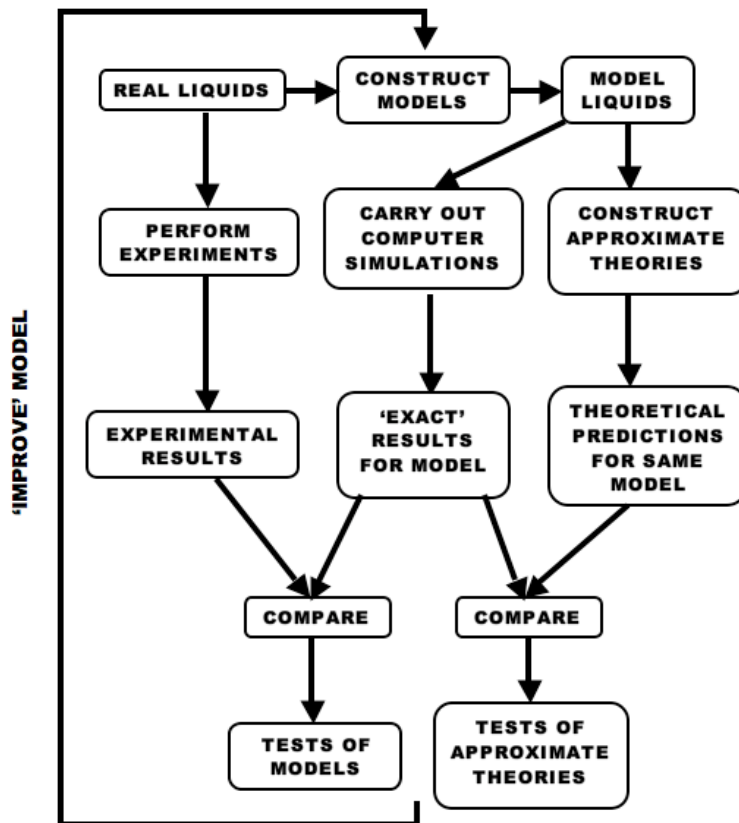


Figure 2.1: The connection between experiment, theory, and computer simulation, adapted from Allen and Tildesley [3].

The experiments might correspond to the determination of thermodynamic properties including phase behavior or to determining the structure of the liquid via scattering techniques. It is, of course, a matter of taste as to whether one implements the last step, i.e. improving the model to make the description of the real liquid more accurate.

2.1 Classical fluids

First we define what we mean by classical fluids. These are fluids for which the thermal de Broglie wavelength $\Lambda = \left(\frac{\beta h^2}{2\pi m}\right)^{1/2} \ll a$, where $\beta = (k_B T)^{-1}$, m is the mass of an atom or particle, and a is the mean atomic spacing. Quantum interference effects are disregarded and the kinetic energy takes its classical value. For example, $\Lambda/a \approx 0.08$ for Argon near its triple point.

2.2 Effective Hamiltonians and Model Fluids

In classical statistical physics the building blocks (particles) are often atoms, ions or molecules. Higher energy (electronic) degrees of freedom have been integrated out.

For the noble (or rare) gases He, Ne, Ar, Kr, and Xe the effective potential $\phi(r)$ between two atoms exhibits repulsion at short distances (from Pauli exclusion of the electrons) and attraction at large distances (from London dispersion forces, i.e. induced dipole-induced dipole forces) so that

$$\phi(r) \approx -\frac{A_6}{r^6}, \quad r \rightarrow \infty \quad (2.1)$$

ignoring retardation effects.

The total potential energy of N atoms is then written as

$$\Phi(\mathbf{r}_1, \mathbf{r}_2, \dots, \mathbf{r}_N) = \sum_{i < j} \phi(|\mathbf{r}_i - \mathbf{r}_j|) + 3 \text{ body} + \dots, \quad (2.2)$$

where \mathbf{r}_i is the coordinate of the i -th atom. The sum over pair potentials ϕ is written explicitly. For the noble gases it is a good (reasonable!) approximation to neglect 3 body and higher contributions. One then has a *pairwise additive* description of the total inter-particle potential which leads one to define a model or effective Hamiltonian as

$$H_N = \sum_{i=1}^N \frac{\mathbf{p}_i^2}{2m} + \sum_{i < j} \phi(|\mathbf{r}_i - \mathbf{r}_j|) + \text{any external potential contribution}, \quad (2.3)$$

where \mathbf{p}_i is the momentum of particle i . For the rare gases ϕ often takes a particular simple form e.g. the Lennard-Jones (LJ) model

$$\phi_{\text{LJ}}(r) = 4\epsilon \left[\left(\frac{\sigma}{r} \right)^{12} - \left(\frac{\sigma}{r} \right)^6 \right], \quad (2.4)$$

where the minimum occurs at $r_{\text{min}} = 2^{1/6}\sigma$ and $\phi(r_{\text{min}}) = -\epsilon$. Cruder models are frequently employed, such as the square-well or hard-sphere model. In plasma physics the one-component classical plasma (OCP), which is simply a system of point (+ve) ions in a uniform compensating background of (-ve) charge, is much used.

The Lennard-Jones and square-well models exhibit solid, liquid and gas phases whereas the hard-sphere model exhibits only a freezing transition to a fcc crystal and the OCP freezes to a bcc crystal (see Lectures by H. Löwen).

2.3 Partition functions and Thermodynamics

The classical canonical partition function for a one component fluid is given by,

$$Z_N(\beta, V) = \frac{h^{-dN}}{N!} \int d\mathbf{p}_1 \int_V d\mathbf{r}_1 \dots \int d\mathbf{p}_N \int_V d\mathbf{r}_N e^{-\beta H_N}, \quad (2.5)$$

with Hamiltonian H_N as above. d is the dimensionality and V is the volume of the system. We can integrate over the momenta to obtain

$$Z_N(\beta, V) = \Lambda^{-dN} Q_N, \quad (2.6)$$

where

$$Q_N = \frac{1}{N!} \int_V d\mathbf{r}_1 \dots \int_V d\mathbf{r}_N e^{-\beta\Phi(\mathbf{r}_1, \dots, \mathbf{r}_N)}, \quad (2.7)$$

is the configurational partition function. Note that the potential energy $\Phi(\mathbf{r}_1, \dots, \mathbf{r}_N)$ may still include an external field contribution.

The Helmholtz free energy is simply

$$F_N(\beta, V) = -\beta^{-1} \ln Z_N. \quad (2.8)$$

Other thermodynamic quantities follows from (2.8). The entropy is

$$S = - \left(\frac{\partial F_N}{\partial T} \right)_V, \quad (2.9)$$

and the pressure is

$$p = - \left(\frac{\partial F_N}{\partial V} \right)_T, \quad (2.10)$$

for a uniform (bulk) fluid. For an ideal (non-interacting) gas, where $\Phi \rightarrow 0$, in $d = 3$

$$\beta F_N = \ln(N! \Lambda^{3N} V^{-N}) = N \ln(\Lambda^3 \rho) - N, \quad (2.11)$$

and the pressure $p_{\text{id}} = \rho \beta^{-1}$ with mean number density $\rho = N/V$. These are the standard results for a uniform ideal classical gas.

The grand canonical ensemble is the most convenient for problems involving inhomogeneous fluids [1]. We consider open systems with fixed temperature T and chemical potential μ . The partition function for the grand canonical ensemble is

$$\Xi(\beta, \mu, T) = \sum_{N=0}^{\infty} e^{\beta\mu N} Z_N(\beta, \mu) = \sum_{N=0}^{\infty} \frac{z^N}{N!} \int_V d\mathbf{r}_1 \dots \int_V d\mathbf{r}_N e^{-\beta\Phi(\mathbf{r}_1, \dots, \mathbf{r}_N)}, \quad (2.12)$$

with $z = \Lambda^{-d} e^{\beta\mu}$ the fugacity or activity.

The grand potential is given by,

$$\Omega = -\beta^{-1} \ln \Xi(\beta, \mu, T), \quad (2.13)$$

which for the case of a uniform fluid, reduces to $\Omega = -pV$. The entropy is

$$S = - \left(\frac{\partial \Omega}{\partial T} \right)_{\mu, V}, \quad (2.14)$$

and the mean number of particles is

$$\langle N \rangle = - \left(\frac{\partial \Omega}{\partial \mu} \right)_{T, V}. \quad (2.15)$$

2.4 Structure and Thermodynamic Properties of Bulk Liquids

In order to understand the structure and thermodynamic properties of liquids it is necessary to introduce the hierarchy of correlation (or distribution) functions. These provide statistical information about the average distribution of particles in the liquid at a given state point. The key quantity for a bulk liquid is the radial distribution function $g(r)$, defined so that $\rho 4\pi r^2 dr g(r)$ is the number of particles in volume $4\pi r^2 dr$ at a distance r from a particle fixed at an origin. Note that since liquids have no long range order $g(r) \rightarrow 1$ as $r \rightarrow \infty$. Also for an ideal gas $g(r) = 1, \forall r$.

The liquid structure factor $S(k)$ is defined in $d = 3$ by

$$S(k) - 1 = \rho \int d\mathbf{r} e^{-i\mathbf{k}\cdot\mathbf{r}} (g(r) - 1) = \rho 4\pi \int_0^\infty dr r^2 \frac{\sin kr}{kr} (g(r) - 1). \quad (2.16)$$

$S(k)$ is extracted from X-ray, neutron or light scattering measurements on bulk liquids[1]. Some properties of the liquid structure factor are: i) $S(k) \rightarrow 1$ as $k \rightarrow \infty$, ii) at $k = 0$, $S(0) = \rho \kappa_T / \beta$, where κ_T is the isothermal compressibility, and iii) for the ideal gas $S(k) = 1, \forall k$.

If the potential energy is pairwise additive as in (2.3) then for a bulk system the internal energy (per particle) is

$$\frac{U}{N} = \frac{3}{2} k_B T + \frac{\rho}{2} \int d\mathbf{r} g(r) \phi(r), \quad (2.17)$$

and the pressure is

$$p = \rho k_B T - \frac{\rho^2}{2} \int d\mathbf{r} g(r) \frac{r}{3} \frac{d\phi(r)}{dr}, \quad (2.18)$$

where $\phi(r)$ is the pair potential and ρ is the mean density. Equation (2.17) is referred to as the energy equation and (2.18) as the virial pressure equation. Together with the compressibility sum rule

$$S(0) = 1 + \rho \int dr (g(r) - 1) = \rho \kappa_T / \beta, \quad (2.19)$$

these exact equations provide three routes to thermodynamics. Note than unlike the energy and virial routes, (2.19) is valid for any one-component fluid; this equation is not restricted to the assumption of pairwise additivity.

The liquid structure factor is intimately related to $c^{(2)}(k)$, the Fourier transform of the pair direct correlation function in a bulk fluid:

$$S(k) = \left(1 - \rho c^{(2)}(k)\right)^{-1}. \quad (2.20)$$

The hierarchy of direct correlation functions will be defined in Chapter 4.

Note that for a hard-sphere fluid with diameter σ , $g^{\text{hs}}(r) = 0$ for $r < \sigma$ and the internal energy reduces to $U/N = 3k_{\text{B}}T/2$, the classical average kinetic energy. The virial pressure takes a simple form:

$$\beta p^{\text{hs}} = \rho + 2\pi\rho^2\sigma^3 g^{\text{hs}}(\sigma^+)/3, \quad (2.21)$$

which follows from (2.18) and the fact that $g(r)e^{\beta\phi(r)}$ is continuous for all pair potentials including hard-spheres [1].

It should be evident that one of the main goals of liquid state theory/simulation is to determine $g(r)$, or its Fourier transform $S(k)$, for a model fluid at a thermodynamic state point or at a sequence of state points. $g(r)$ provides basic information about the (average) structure and, if the model is pairwise additive, determines the thermodynamics. Ref [1] provides several examples of $g(r)$ and $S(k)$ for model fluids, comparing results of theory and simulations, and describes experimental results for these quantities.

Chapter 3

Introducing Equilibrium Classical DFT

Classical density functional theory provides a framework for determining thermodynamic properties and correlation functions of a wide variety of *inhomogeneous* (model) fluids starting from a microscopic basis, i.e. the Hamiltonian describing interactions between particles.

DFT is based on the result that the grand potential of a specified inhomogeneous fluid is a functional of the average one-body density,

$$\rho(\mathbf{r}) = \langle \hat{\rho}(\mathbf{r}) \rangle = \left\langle \sum_{i=1}^N \delta(\mathbf{r} - \mathbf{r}_i) \right\rangle, \quad (3.1)$$

where \mathbf{r}_i is the position coordinate of particle i .

Minimizing the grand potential functional w.r.t. $\rho(\mathbf{r})$ determines the equilibrium density profile and free energy and further derivatives provide correlation functions.

The structure and the thermodynamic properties of inhomogeneous fluids, where the average density $\rho(\mathbf{r})$ is spatially varying, are generally much more difficult to determine than is the case for homogeneous fluids where ρ is constant. Theories developed for the latter do not necessarily lend themselves easily to inhomogeneous fluids where the spatial variation of $\rho(\mathbf{r})$ is usually set by that of the external potential $V(\mathbf{r})$. Of course, the overall strategy and motivation is much the same as in Figure 2.1—one is still considering the properties of liquids but now new phenomena, including new phase transitions, occur because translational invariance is broken either by the presence of an external field or spontaneously when a fluid-crystal (freezing) transition can take place. Classical DFT focuses on finding approximations, directly or indirectly, for the grand potential functional. In this sense classical DFT mimics electronic (fermionic) DFT where the strategy is to find suitable approximations for the grand potential functional of the average electron density $n(\mathbf{r})$. Indeed classical DFT has its origins in electronic DFT, e.g. Ref [5]

There are several advantages of using DFT rather than other techniques of liquid state physics. Methods of functional differentiation yield formally exact results more

readily and elegantly than methods focussing on the partition function Ξ , e.g. important sum rules that link thermodynamic functions to structure. For a (model) fluid with a given effective interatomic potential $\Phi(\mathbf{r}_1, \dots, \mathbf{r}_N)$ one can devise approximations for the intrinsic Helmholtz functional $\mathcal{F}[\rho]$ that should be applicable to all inhomogeneities. The key idea is that $\mathcal{F}[\rho]$ is a unique functional of $\rho(\mathbf{r})$; its form does not depend on the external potential $V(\mathbf{r})$. The same functional $\mathcal{F}[\rho]$ should be valid for fluids adsorbed at walls, confined in pores or in ‘strong’ gravitational fields or indeed for a crystal where $\rho(\mathbf{r})$ is periodic. Moreover, from a practical perspective, it is straightforward to incorporate dispersion forces, important at mesoscopic length scales, into DFT. Long-ranged potentials are not easily incorporated into simulations

DFT also has disadvantages and pitfalls. Different types of fluid require different approximate functionals. Skill and intuition are required to construct $\mathcal{F}[\rho]$ for a particular model fluid; systematic approaches are few and are often not well-suited to certain types of inhomogeneity-especially when determining phase behavior. Approximate functionals will very often omit fluctuation effects. It can be tempting to regard a specified $\mathcal{F}[\rho]$ as defining some model fluid. Of course this is dangerous unless the functional is known exactly, which is the case only for hard-rods in $d = 1$. One can easily lose sight of the underlying model Hamiltonian. We return to these issues in Section 5.1 after we have summarized the formal structure of classical DFT.

Chapter 4

Summary of DFT Formalism for a Simple Fluid

In this section we summarize the formal structure of classical DFT, specializing to a single component fluid. We work in the grand canonical ensemble as this is usually the most convenient for treating inhomogeneous fluids. Generalization to mixtures, i.e. multicomponent fluids, is straightforward.

This section draws heavily on the presentation of DFT given in the review article by the present author [5]. We omit formal proofs. Some of these, can be found in an early articles [6, 7] or in the text book [1]. Rigorous treatments of classical DFT are given in [8, 9].

4.1 Generating Functionals and Hierarchies of Correlation Functions

The Hamiltonian for the fluid of N atoms or particles, each of mass m , is

$$\begin{aligned} H_N &= \sum_{i=1}^N \frac{\mathbf{p}_i^2}{2m} + \Phi(\mathbf{r}_1, \dots, \mathbf{r}_N) + \sum_{i=1}^N V(\mathbf{r}_i) \\ &\equiv \text{K.E.} \quad + \Phi \quad \quad \quad + V, \end{aligned} \tag{4.1}$$

where \mathbf{p}_i is the momentum of atom i and Φ now denotes the total interatomic potential energy. The latter is not necessarily pairwise additive. The one-body external potential $V(\mathbf{r})$ is, as yet, arbitrary. The grand potential $\Omega = -\beta^{-1} \ln \Xi$, where Ξ is the partition function, is a function of chemical potential μ , inverse temperature $\beta = (k_B T)^{-1}$, and the available volume; it is also a functional of $V(\mathbf{r})$ and therefore of the combination

$$u(\mathbf{r}) \equiv \mu - V(\mathbf{r}). \tag{4.2}$$

A hierarchy of correlation functions is obtained by functional differentiation of Ω with respect to $u(\mathbf{r})$. The first derivative is the average one-body density,

$$\rho(\mathbf{r}) \equiv \rho^{(1)}(\mathbf{r}) \equiv \langle \hat{\rho}(\mathbf{r}) \rangle = -\frac{\delta\Omega}{\delta u(\mathbf{r})}, \quad (4.3)$$

where $\hat{\rho}(\mathbf{r}) = \sum_{i=1}^N \delta(\mathbf{r} - \mathbf{r}_i)$ is the density ‘operator’ and $\langle \rangle$ denotes the ensemble average. The latter is defined for an arbitrary ‘operator’ \hat{O} by

$$\langle \hat{O} \rangle \equiv \text{Tr}_{\text{cl}} f_N \hat{O}, \quad (4.4)$$

where f_N is the probability density

$$f_N = \Xi^{-1} \exp[-\beta(H_N - \mu N)]. \quad (4.5)$$

As usual the classical trace is defined by

$$\text{Tr}_{\text{cl}} \equiv \sum_{N=0}^{\infty} \frac{1}{h^{3N} N!} \int d\mathbf{r}_1 \dots \int d\mathbf{r}_N \int d\mathbf{p}_1 \dots \int d\mathbf{p}_N. \quad (4.6)$$

For a fluid $\rho(\mathbf{r})$ must have the symmetry of the external potential $V(\mathbf{r})$. A second derivative yields the (two-body) density-density correlation function

$$\begin{aligned} G(\mathbf{r}_1, \mathbf{r}_2) &\equiv \langle (\hat{\rho}(\mathbf{r}_1) - \langle \hat{\rho}(\mathbf{r}_1) \rangle) (\hat{\rho}(\mathbf{r}_2) - \langle \hat{\rho}(\mathbf{r}_2) \rangle) \rangle \\ &= \beta^{-1} \frac{\delta \rho(\mathbf{r}_1)}{\delta u(\mathbf{r}_2)} = -\beta^{-1} \frac{\delta^2 \Omega}{\delta u(\mathbf{r}_2) \delta u(\mathbf{r}_1)}, \end{aligned} \quad (4.7)$$

which is related to the two-body distribution function $\rho^{(2)}$ of liquid state theory [1] via

$$G(\mathbf{r}_1, \mathbf{r}_2) = \rho^{(2)}(\mathbf{r}_1, \mathbf{r}_2) - \rho(\mathbf{r}_1)\rho(\mathbf{r}_2) + \rho(\mathbf{r}_1)\delta(\mathbf{r}_1 - \mathbf{r}_2). \quad (4.8)$$

Further differentiation yields three-body, four-body, and so on, density-density correlation functions. This procedure of generating correlation functions by differentiation w.r.t. external potentials is the standard one in equilibrium statistical mechanics. Note that for a bulk fluid of uniform density ρ , $\rho(\mathbf{r}) \rightarrow \rho$ and translational invariance demands that $G(\mathbf{r}_1, \mathbf{r}_2) = \rho^2(g(r_{12}) - 1) + \rho\delta(r_{12})$, where $r_{12} \equiv |\mathbf{r}_1 - \mathbf{r}_2|$ and $g(r)$ is the usual radial distribution function. It follows that the Fourier transform $G(k) = \rho S(k)$, where $S(k)$ is the static structure factor of the bulk liquid mentioned in Section 2.4.

The density functional approach focuses on functionals of $\rho(\mathbf{r})$ rather than of $u(\mathbf{r})$. Whilst it is clear that $\rho(\mathbf{r})$ is a functional of $u(\mathbf{r})$, one can prove [6, 7, 8, 9] the less obvious result that for given Φ , μ , and T the probability density is uniquely determined by $\rho(\mathbf{r})$ —the latter fixes $V(\mathbf{r})$, which then determines f_N . The proof proceeds by considering first the grand potential as a functional of a probability density f , normalized so that $\text{Tr}_{\text{cl}} f = 1$, and then showing by means of a Gibbs inequality that $\Omega[f] > \Omega[f_N] \equiv \Omega$. The next step is to use this inequality to show that two different external potentials cannot give rise to the same equilibrium one-body density profile $\rho(\mathbf{r})$, i.e. there is only

one external potential that gives rise to a specified density profile. It follows that since f_N is a unique functional of $\rho(\mathbf{r})$, so is the quantity

$$\begin{aligned}\mathcal{F}[\rho] &\equiv \langle \text{K.E.} + \Phi + \beta^{-1} \ln f_N \rangle \\ &= \text{Tr}_{\text{cl}}[f_N(\text{K.E.} + \Phi + \beta^{-1} \ln f_N)].\end{aligned}\quad (4.9)$$

The same form of $\mathcal{F}[\rho]$ will be valid for any external potential. A second functional is constructed from a Legendre transform of \mathcal{F} :

$$\Omega_V[\tilde{\rho}] = \mathcal{F}[\tilde{\rho}] - \int d\mathbf{r} u(\mathbf{r}) \tilde{\rho}(\mathbf{r}), \quad (4.10)$$

where the external potential is fixed and $\tilde{\rho}(\mathbf{r})$ is an average one-body density. When $\tilde{\rho} = \rho$, the equilibrium density, $\Omega_V[\tilde{\rho}]$, reduces to the grand potential Ω . Moreover Ω is the minimum value of $\Omega_V[\tilde{\rho}]$, so that we have a variational principle

$$\left. \frac{\delta \Omega_V[\tilde{\rho}]}{\delta \tilde{\rho}(\mathbf{r})} \right|_{\tilde{\rho}=\rho} = 0, \quad \Omega_V[\rho] = \Omega, \quad (4.11)$$

for determining the equilibrium density of a fluid in an external potential. $\mathcal{F}[\rho]$ is the intrinsic Helmholtz free-energy functional, since the total Helmholtz free energy $F = \Omega + \mu \int d\mathbf{r} \rho(\mathbf{r}) = \mathcal{F}[\rho] + \int d\mathbf{r} \rho(\mathbf{r}) V(\mathbf{r})$. Combining (4.10) and (4.11) we have

$$\mu = V(\mathbf{r}) + \frac{\delta \mathcal{F}[\rho]}{\delta \rho(\mathbf{r})}, \quad (4.12)$$

which expresses the constancy of the chemical potential μ through the inhomogeneous fluid. Clearly $\delta \mathcal{F}[\rho]/\delta \rho(\mathbf{r})$ can be regarded as the intrinsic chemical potential; in general this will not be a local function of $\rho(\mathbf{r})$. It will include an ideal-gas term $\beta^{-1} \ln \Lambda^3 \rho(r)$ and a term arising from interactions between the particles.

By virtue of (4.11), use of $\Omega_V[\rho]$ as a generating functional by differentiating w.r.t. $u(\mathbf{r})$ is identical to the standard procedure. A second hierarchy of correlation functions is generated by differentiating $\mathcal{F}[\rho] = \mathcal{F}_{\text{id}}[\rho] + \mathcal{F}_{\text{ex}}[\rho]$. The ideal gas (non-interacting) contribution is

$$\mathcal{F}_{\text{id}}[\rho] = \int d\mathbf{r} f_{\text{id}}(\rho(\mathbf{r})), \quad (4.13)$$

with $f_{\text{id}}(\rho) = \beta^{-1} \rho (\ln \Lambda^3 \rho - 1)$, the free-energy density of a uniform ideal gas-see (2.11). Thus we generate the *direct correlation* function hierarchy:

$$c^{(1)}(\mathbf{r}) = -\frac{\delta(\beta \mathcal{F}_{\text{ex}}[\rho])}{\delta \rho(\mathbf{r})} \equiv -\frac{\delta(\beta \mathcal{F}[\rho] - \beta \mathcal{F}_{\text{id}}[\rho])}{\delta \rho(\mathbf{r})}, \quad (4.14)$$

$$c^{(2)}(\mathbf{r}_1, \mathbf{r}_2) = \frac{\delta c^{(1)}(\mathbf{r}_1)}{\delta \rho(\mathbf{r}_2)} = -\frac{\delta^2(\beta \mathcal{F}_{\text{ex}}[\rho])}{\delta \rho(\mathbf{r}_2) \delta \rho(\mathbf{r}_1)} = c^{(2)}(\mathbf{r}_2, \mathbf{r}_1), \quad (4.15)$$

that is

$$c^{(n)}(\mathbf{r}_1, \dots, \mathbf{r}_2) = \frac{\delta c^{(n-1)}(\mathbf{r}_1, \dots, \mathbf{r}_{n-1})}{\delta \rho(\mathbf{r}_n)},$$

where the tilde in the density variable is omitted. $\mathcal{F}_{\text{ex}}[\rho]$ is the excess (over ideal) Helmholtz free energy functional arising from the interactions. Using (4.13) and (4.14), equation (4.12) may be re-expressed as

$$\Lambda^3 \rho(\mathbf{r}) = \exp[\beta u(\mathbf{r}) + c^{(1)}(\mathbf{r})], \quad (4.16)$$

where $c^{(1)}$ is itself a functional of $\rho(\mathbf{r})$. For an ideal gas $c^{(1)} \equiv 0$ and (4.16) reduces to the familiar barometric law for the density distribution in the presence of an external field. Thus (4.16) implies that $-\beta^{-1}c^{(1)}(\mathbf{r})$ acts as an additional effective one-body potential in determining self-consistently the equilibrium density. This quantity is the classical analog of the effective one-body potential $\int d\mathbf{r}' n(\mathbf{r}')/|\mathbf{r} - \mathbf{r}'| + \delta E_{\text{xc}}[n]/\delta n(\mathbf{r})$ entering the Kohn and Sham theory [10] for the electron density $n(\mathbf{r})$, where $E_{\text{xc}}[n]$ is the exchange-correlation functional. That potential enters a one-electron Schrödinger equation appropriate to a noninteracting electron liquid. The presence of the exponential in (4.16) reflects the corresponding classical behavior, i.e. the form of the barometric law is retained.

In a uniform fluid with $V(\mathbf{r}) \equiv 0$, (4.16) reduces to

$$\mu(\rho) = \mu_{\text{id}}(\rho) - \beta^{-1}c^{(1)}(\rho), \quad (4.17)$$

with $\mu_{\text{id}}(\rho) = df_{\text{id}}/d\rho = \beta^{-1} \ln \Lambda^3 \rho$, so that $c^{(1)}(\rho)$ is proportional to the excess (over ideal) chemical potential. Equation (4.16) is also equivalent to Widom's potential distribution formula, as pointed out by Henderson [11]. From (4.14), (4.15) and (4.12) we find that

$$c^{(2)}(\mathbf{r}_1, \mathbf{r}_2) = \frac{\delta(\mathbf{r}_1 - \mathbf{r}_2)}{\rho(\mathbf{r}_1)} - \beta \frac{\delta u(\mathbf{r}_1)}{\delta \rho(\mathbf{r}_2)}, \quad (4.18)$$

where the second term is [via (4.7)] $-G^{-1}(\mathbf{r}_1, \mathbf{r}_2)$, the functional inverse being defined as

$$\int d\mathbf{r}_3 G^{-1}(\mathbf{r}_1, \mathbf{r}_3) G(\mathbf{r}_3, \mathbf{r}_2) = \delta(\mathbf{r}_1 - \mathbf{r}_2). \quad (4.19)$$

thus $c^{(2)}$ is (essentially) the inverse of the density-density correlation function G . With (4.8), (4.18) and (4.19) together imply the integral equation

$$h(\mathbf{r}_1, \mathbf{r}_2) = c^{(2)}(\mathbf{r}_1, \mathbf{r}_2) + \int d\mathbf{r}_3 h(\mathbf{r}_1, \mathbf{r}_3) \rho(\mathbf{r}_3) c^{(2)}(\mathbf{r}_3, \mathbf{r}_2), \quad (4.20)$$

relating the two-body direct correlation function $c^{(2)}$ of the inhomogeneous fluid to the *total* correlation function h defined by

$$\rho(\mathbf{r}_1) \rho(\mathbf{r}_2) h(\mathbf{r}_1, \mathbf{r}_2) \equiv \rho^{(2)}(\mathbf{r}_1, \mathbf{r}_2) - \rho(\mathbf{r}_1) \rho(\mathbf{r}_2). \quad (4.21)$$

Equation (4.20) is the familiar Ornstein-Zernike equation for an inhomogeneous fluid [1, 5]. Often this is used to define $c^{(2)}$. However, we see that this equation follows as a natural consequence of having two generating functionals Ω_V and \mathcal{F} linked by the Legendre transform (4.10); that is, (4.19) is equivalent to

$$\int d\mathbf{r}_3 \frac{\delta^2 \mathcal{F}}{\delta \rho(\mathbf{r}_1) \delta \rho(\mathbf{r}_3)} \frac{\delta^2 \Omega_V}{\delta u(\mathbf{r}_3) \delta u(\mathbf{r}_2)} = -\delta(\mathbf{r}_1 - \mathbf{r}_2). \quad (4.22)$$

Thus the direct correlation function hierarchy has equal status with the standard distribution function hierarchy of liquid state theory [1, 5]. Indeed, the existence of two hierarchies, generated by two generating functionals, is a common procedure in many-body theory. In field theoretical treatments [12] of statistical mechanics, the analog of $\mathcal{F}[\rho]$ is $\Gamma[\bar{\Phi}]$, the generating functional for the vertex functions $\Gamma^{(N)}$, with $\bar{\Phi}$, the *averaged* order parameter, being the analog of the average density $\rho(\mathbf{r})$.

An excellent review by Henderson [11] describes how this DFT formalism can be used to derive several exact sum rules linking correlation functions to thermodynamic quantities in inhomogeneous fluids.

4.2 The Free-Energy via Integration

There are several routes to the calculation of the free energy of an inhomogeneous fluid [7]. Here we describe one of these. Consider an initial fluid state with density $\rho_i(\mathbf{r})$ and a final state with density $\rho(\mathbf{r})$ at the same temperature T and suppose that these can be linked by a linear path in the space of density functions characterized by a single coupling parameter α :

$$\begin{aligned}\rho_\alpha \equiv \rho(\mathbf{r}; \alpha) &= \rho_i(\mathbf{r}) + \alpha(\rho(\mathbf{r}) - \rho_i(\mathbf{r})) \\ &\equiv \rho_i(\mathbf{r}) + \alpha\Delta\rho(\mathbf{r}),\end{aligned}\tag{4.23}$$

with $0 \leq \alpha \leq 1$. Integration of (4.14) yields

$$\beta\mathcal{F}_{\text{ex}}[\rho] = \beta\mathcal{F}_{\text{ex}}[\rho_i] - \int_0^1 d\alpha \int d\mathbf{r} \Delta\rho(\mathbf{r}) c^{(1)}([\rho_\alpha; \mathbf{r}]),\tag{4.24}$$

where the functional dependence of $c^{(1)}$ is made explicit. A second integration [see (4.15)] gives

$$c^{(1)}([\rho_\alpha; \mathbf{r}_1) = c^{(1)}([\rho_i; \mathbf{r}_1) + \int_0^\alpha d\alpha' \int d\mathbf{r}_2 \Delta\rho(\mathbf{r}_2) c^{(2)}([\rho_{\alpha'}; \mathbf{r}_1, \mathbf{r}_2).\tag{4.25}$$

For a uniform fluid (4.25) simplifies, with $\rho_i \equiv 0$, to

$$c^{(1)}(\rho) = \int_0^\rho d\rho' \int d\mathbf{r}_2 c^{(2)}(\rho'; \mathbf{r}_1, \mathbf{r}_2),\tag{4.26}$$

so that

$$\frac{\partial c^{(1)}(\rho)}{\partial \rho} = \int d\mathbf{r} c^{(2)}(\rho; r),\tag{4.27}$$

which, by virtue of (4.17), is equivalent to

$$\beta\rho \left(\frac{\partial \mu}{\partial \rho} \right)_T = 1 - \rho \int d\mathbf{r} c^{(2)}(\rho; r).\tag{4.28}$$

This equation is simply a statement of the compressibility sum rule as $c^{(2)}(\rho; \mathbf{r}_1, \mathbf{r}_2) \equiv c^{(2)}(\rho; |\mathbf{r}_1 - \mathbf{r}_2|)$ is the (two-body) direct correlation function of the bulk fluid-see (2.19) and (2.20). Equations (4.24) and (4.25) can be combined to give

$$\begin{aligned} \beta \mathcal{F}_{\text{ex}}[\rho] &= \beta \mathcal{F}_{\text{ex}}[\rho_i] - \int d\mathbf{r} \Delta\rho(\mathbf{r}) c^{(1)}([\rho_i]; \mathbf{r}) \\ &- \int_0^1 d\alpha \int d\mathbf{r}_1 \Delta\rho(\mathbf{r}_1) \int_0^\alpha d\alpha' \int d\mathbf{r}_2 \Delta\rho(\mathbf{r}_2) c^{(2)}([\rho_{\alpha'}]; \mathbf{r}_1, \mathbf{r}_2). \end{aligned} \quad (4.29)$$

As emphasized by Saam and Ebner [13] this result should be independent of the choice (4.23) of integration path; recall that $\mathcal{F}_{\text{ex}}[\rho]$ is a unique functional of $\rho(\mathbf{r})$. A more familiar version of (4.29) emerges when $\rho_i \equiv 0$ and the final state is a uniform fluid of density ρ . The total Helmholtz free energy density is

$$f(\rho) = f_{\text{id}}(\rho) + \beta^{-1} \rho^2 \int_0^1 d\alpha (\alpha - 1) \int d\mathbf{r} c^{(2)}(\alpha\rho; r), \quad (4.30)$$

where an identity has been used to reduce the double integration over α and α' to a single integration [5]. Use of (4.30) requires integration paths in a single phase region.

Note that (4.29) is the starting point for the modern theory of freezing. The initial reference state is a bulk liquid and the final state is a bulk crystal-viewed as an inhomogeneous fluid. This approach requires the two-body direct correlation function, $c^{(2)}$, as a functional of $\rho(\mathbf{r})$ and approximations must be made. Some of these are described in the lectures of Löwen at this School.

4.3 Hard Rods in One Dimension: An Exactly Solvable Model

There is no continuum model for which the statistical mechanics can be solved exactly in three dimensions. Thus there is no model for which the functional $\mathcal{F}[\rho]$ is known exactly in three dimensions. In one dimension, however, exact results do exist for particles with nearest-neighbor interactions. Percus [14] derived an integral equation for the density profile $\rho(z)$ of a one-dimensional fluid of hard rods (length σ) in an arbitrary external potential $V(z)$ via functional differentiation of the grand partition function with respect to $u(z) \equiv \mu - V(z)$. Robledo [15] obtained the same equation from potential distribution theory, while Robledo and Varea [16] and Percus [17] constructed the functional $\Omega_V[\rho]$. This is

$$\Omega_V[\rho] = \mathcal{F}_{\text{id}}[\rho] + \mathcal{F}_{\text{ex}}[\rho] - \int dz u(z) \rho(z), \quad (4.31)$$

with the excess free-energy functional for hard rods in one dimension given by

$$\mathcal{F}_{\text{ex}}[\rho] \equiv \mathcal{F}_{\text{ex}}^{\text{hr}} = \beta^{-1} \int dz \rho(z) \ln[1 - t(z)], \quad (4.32)$$

where $t(z) = \int_{z-\sigma}^z dy \rho(y)$. Requiring $\Omega_V[\rho]$ to be minimum yields Percus's equation for the profile:

$$\beta u(z) = \ln \frac{\Lambda \rho(z)}{1 - t(z)} + \int_z^{z+\sigma} dy \frac{\rho(y)}{1 - t(y)}. \quad (4.33)$$

$c^{(2)}$, $c^{(3)}$, and so on, can be obtained by further functional differentiation and can be shown [14] to be of finite range in all pairs of variables [e.g., $c^{(2)}(z, z') = 0$ unless $|z - z'| \leq \sigma$]. Percus [17] also considered the case of sticky hard rods, deriving $\Omega_V[\rho]$ and showing that $c^{(2)}$ vanishes beyond the range of the core. For the special case of hard rods confined by two hard walls, Robledo and Rowlinson [18] have obtained a complete set of results, including the n -body distribution functions and the solvation force (the excess pressure brought about by confinement). Vanderlick et. al. [19] have extended the work of Percus to mixtures of hard rods in an arbitrary external field, and these authors provide many results for density profiles, selective adsorption, and solvation force of a binary mixture confined between two walls.

Do these exact solutions guide us toward an effective approximation for fluids in higher dimensions? This question was posed by Percus [17] and Robledo and Varea [16], who suggested possible approximation schemes for higher dimensions based on (4.32). The excess free energy functional for hard-rod mixtures can be written as

$$\beta \mathcal{F}_{\text{ex}}^{\text{hr}}[\{\rho_i\}] = \int dz \Phi^{\text{hr}}(\{n_\alpha(z)\}), \quad (4.34)$$

where ρ_i is the average density profile of species i , with $i = 1, 2, \dots, \nu$. The 'radius' of species i is R_i so that the length of a rod of species i is $2R_i$. $\beta^{-1} \Phi^{\text{hr}}$ is the excess free energy density which is a *function*, not a functional, of a set of weighted densities n_α . The latter are defined by

$$n_\alpha(z) = \sum_{i=1}^{\nu} \int dz' \rho_i(z') w_i^{(\alpha)}(z - z'), \quad (4.35)$$

i.e. sums over all species of convolutions of the actual density with weight functions $w_i^{(\alpha)}$ that are specific to the geometry of species i . In this one dimensional case there are two different weight functions for each species, namely

$$w_i^{(0)}(z) = \frac{1}{2}(\delta(z - R_i) + \delta(z + R_i)), \quad (4.36)$$

that is associated with the ends (the 'surface') of the rod, and

$$w_i^{(1)}(z) = \Theta(R_i - |z|), \quad (4.37)$$

that can be associated with the 'volume' of the rod.

The free energy density is given by

$$\Phi^{\text{hr}}(n_\alpha) = -n_0 \ln(1 - n_1), \quad (4.38)$$

and one should note that the excess free energy per particle of a uniform hard-rod fluid of density ρ is

$$\psi_{\text{ex}}^{\text{hr}}(\rho) = -\beta^{-1} \ln(1 - \rho\sigma). \quad (4.39)$$

It is straightforward to show that (4.34) reduces to (4.32) for the one-component case with $\sigma = 2R$.

That the exact one-dimensional hard-rod free energy functional should possess such a simple structure is remarkable and was an important ingredient in motivating Rosenfeld's Fundamental Measures Theory (FMT) of hard-sphere mixtures [20]. The FMT functional has the same form as (4.34) but now with weighted densities that are convolutions of the density profiles with weight functions depending on the geometrical properties of the spheres. We return to Rosenfeld's FMT in Section 5.3.1.

Chapter 5

Approximate Free Energy Functionals

5.1 The Strategy and its Shortcomings

As emphasized in earlier Sections, most applications of DFT are based upon an explicit approximation for the functional $\mathcal{F}[\rho]$. Once this is given, the equilibrium density profile $\rho(\mathbf{r})$ and grand potential Ω are determined by minimization of the corresponding $\Omega_V[\rho]$, i.e. by (4.10) and (4.11), for specified T , μ and external potential $V(\mathbf{r})$.

A second functional differentiation yields the (approximate) two-body direct correlation function $c^{(2)}$ and the density-density correlation function $G(\mathbf{r}_1, \mathbf{r}_2)$ follows from the Ornstein-Zernike equation (4.19) or (4.20). From a pragmatic viewpoint this strategy is appealing. The reliability and accuracy of the results should reflect the skill with which $\mathcal{F}[\rho]$ is constructed for the particular model Hamiltonian. For certain problems one might be able to extract understanding of the essential phenomena using very crude approximations. For others, which demand detailed information about the microscopic structure, sophisticated approximations will be required. From a more fundamental statistical mechanics viewpoint the strategy is less satisfactory. There is always great danger of losing sight of the Hamiltonian. Once $\mathcal{F}[\rho]$ is specified, all equilibrium properties are determined, so there is a temptation to regard $\mathcal{F}[\rho]$ as defining some model fluid. If $\mathcal{F}[\rho]$ corresponds to some exactly solved model, as in the case of hard rods, there is a one-to-one relationship between the functional and the Hamiltonian. If, however, $\mathcal{F}[\rho]$ is merely some (intelligently chosen) functional, there is no reason to expect the resulting properties to be those which would correspond to exact solution of *any* Hamiltonian, let alone the original [5].

Phase transitions warrant particular attention. We cannot expect any approximate density functional treatment to provide a full description of phase transitions. Most approximate functionals are mean field in character, so that certain (but not all) effects of fluctuations will necessarily be omitted. An important case is that of a fluid-fluid interface in a weak gravitational field where thermal capillary-wave-like fluctuations play a role. DFT treatments omit the fluctuation-induced broadening of the interfacial

density profile; these shortcomings of DFT are discussed in Ref. [5]-see Section 5. Since most DFT approaches treat attractive interactions in mean-field fashion they do not account properly for bulk critical fluctuations, i.e. these associated with a diverging bulk correlation length, and the critical exponents take their mean-field values.

It is worth pointing out the difference between the density functional strategy and the more conventional field-theoretical approach. There one does not normally make *direct* approximations to the generating functional $\Gamma[\bar{\Phi}]$; rather, one uses the machinery of loop expansions, etc., to generate systematic approximations for thermodynamic functions and correlation functions [12]. This usually allows one to keep track of fluctuation effects. However, field-theoretical treatments of realistic models of inhomogeneous fluids are not easy! By approximating $\Gamma[\bar{\Phi}]$ (or $\mathcal{F}[\rho]$) directly it is sometimes difficult to ascertain what, if any, fluctuation effects are being incorporated into the theory. The well-known Fisk-Widom [21] theory of the liquid-gas interface near the bulk critical point is in this spirit. Although their functional omits interfacial (capillary-wave induced) broadening of the density profile, it is constructed so as to incorporate the effects of bulk critical fluctuations, i.e. the correct bulk critical exponents.

The classical density functional strategy is very much in keeping with that used for electronic properties. In the Hohenberg-Kohn-Sham scheme the analog of $\mathcal{F}_{\text{ex}}[\rho]$ is the energy functional

$$\frac{1}{2} \int \int d\mathbf{r} d\mathbf{r}' \frac{n(\mathbf{r})n(\mathbf{r}')}{|\mathbf{r} - \mathbf{r}'|} + E_{\text{xc}}[n],$$

and approximations are sought for $E_{\text{xc}}[n]$. Simple Hartree theory sets $E_{\text{xc}}[n] = 0$, and includes only the explicit electrostatic energy. For classical atomic fluids where the pairwise potential $\phi(r)$ has both repulsive and attractive contributions the division of $\mathcal{F}_{\text{ex}}[\rho]$ is not so obvious. For ionic liquids, however, it is natural to separate out the total electrostatic energy and seek approximations for the remaining part of \mathcal{F}_{ex} , which is then the classical analog of the exchange and correlation functional $E_{\text{xc}}[n]$. Note that the Poisson-Boltzmann theory of charged fluids is equivalent to including only the electrostatic contribution to \mathcal{F}_{ex} , see e.g. [22].

In the remainder of this section we describe various approximations for $\mathcal{F}[\rho]$, some generic and others specific to particular model fluids.

5.2 Two Generic Examples

5.2.1 Square-Gradient Approximation

The best known approximation is probably that arising from truncating the gradient expansion of $\mathcal{F}_{\text{ex}}[\rho]$. This is derived by supposing that the density $\rho(\mathbf{r}) \equiv \Psi(\mathbf{r}/r_0)$, where the scale parameter $r_0 \rightarrow \infty$. Then the density may vary by large amounts but over a long distance scale. One finds [7]:

$$\mathcal{F}_{\text{ex}}[\rho] = \int d\mathbf{r} [f_{\text{ex}}(\rho(\mathbf{r})) + f_2(\rho(\mathbf{r}))(\nabla\rho(\mathbf{r}))^2 + O(\nabla\rho)^4]. \quad (5.1)$$

Successive terms correspond to successive powers of r_0^{-1} and symmetry arguments, equivalent to those used in Landau theory, eliminate certain terms. $f_{\text{ex}}(\rho)$ is the excess Helmholtz free-energy density of a uniform fluid of density ρ , so that truncating the expansion after the first term constitutes the local density approximation. Note that the exact ideal gas contribution (4.13) does have local density form. The other coefficients, $f_2(\rho)$, and so on, can only be determined by imposing additional requirements on $\mathcal{F}_{\text{ex}}[\rho]$. A natural choice is that (5.1) should be consistent with linear response theory, i.e. with the change of free energy obtained by creating an infinitesimal perturbation of the density $\delta\rho(\mathbf{r})$ away from that of a uniform fluid. That change can be obtained by functional Taylor expansion and involves the direct correlation functions of the uniform fluid [7]. It is found that

$$f_2(\rho) = (12\beta)^{-1} \int d\mathbf{r} r^2 c^{(2)}(\rho; r). \quad (5.2)$$

Higher-order coefficients depend on integrals of $c^{(n)}$ with $n > 2$ and are much less amenable to calculation. For this reason and for overall simplicity (5.1) is usually truncated after the second term. With some means (e.g., via integral equation or perturbation theory) of calculating $c^{(2)}(\rho; r)$, and hence $f_{\text{ex}}(\rho)$ and $f_2(\rho)$, for bulk fluids (5.1) constitutes a very simple but fully microscopic theory for an inhomogeneous fluid.

Formally, the square-gradient approximation should be valid only for the case of very slowly varying density profiles, such as would pertain for the fluid-fluid interface near the bulk critical point or for a (single phase) fluid in a gravitational field.

The neglect of higher-order terms in the expansion has severe repercussions when the theory is employed for fluids with power-law decaying pairwise potentials $\phi(r)$. A formal gradient expansion does not exist for such potentials. Since $c^{(2)}(\rho; r) \sim -\beta\phi(r)$ as $r \rightarrow \infty$, higher moments of $c^{(2)}$ will diverge if $\phi(r) \sim -r^{-n}$ as $r \rightarrow \infty$. The most relevant case is the Lennard-Jones 12-6 potential, which has $n = 6$. $f_2(\rho)$ exists but not higher-order coefficients. This is reflected in the small k behaviour of the Fourier transform $c^{(2)}(\rho; k)$, where the presence of a k^3 term reflects the $-r^{-6}$ decay of $\phi(r)$ [23, 24]. The square-gradient approximation fails to describe the z^{-3} algebraic decay of the tails of $\rho(z)$ at the liquid-gas interface of the Lennard-Jones fluid [25]; rather, it predicts exponential decay. More important, it cannot account for the proper divergence of the wetting film thickness in systems that exhibit dispersion (van der Waals) forces. Such difficulties are best surmounted by treating attractive forces in a nonlocal fashion that avoids the gradient expansion. In the extreme case of an ionic liquid ($n = 1$) a gradient expansion is meaningful only for the residual, non-Coulombic, part of $\mathcal{F}_{\text{ex}}[\rho]$ [26].

There is another difficulty associated with the implementation of (5.1) with (5.2). If the fluid exhibits attractive, as well as repulsive interatomic forces, bulk liquid-gas coexistence may occur. The density of the inhomogeneous fluid may take values locally that lie within the bulk two-phase region. This is certainly the case for many interfacial problems. One must decide what values should be used for the free energy density $f(\rho)$, and how to calculate $c^{(2)}(\rho; r)$. In practice, $f(\rho)$ always has some (generalized) van der Waals form, so that $\mu(\rho) = \partial f / \partial \rho$ has a loop for subcritical temperatures. Some

extrapolation of $c^{(2)}(\rho; r)$ [or $f_2(\rho)$] into the two-phase region is usually made. For the Lennard-Jones fluid, $f_2(\rho)$ is calculated to be weakly density and temperature dependent. The integral in (5.2) is dominated by the larger r portion, where $c^{(2)}(\rho; r) \sim -\beta\phi(r)$ and f_2 can be regarded as a positive constant determined primarily by the attractive part of $\phi(r)$. The resulting square-gradient theory is then essentially the same as that used by van der Waals in his classic theory of the liquid-gas interface [27, 7].

Despite the shortcomings described above, the square-gradient approximation has proved extremely valuable for a wide variety of interfacial problems, including Cahn's [28] seminal paper on wetting transitions. These applications are reviewed briefly in Refs. [5, 29].

5.2.2 Density Expansions

Consider the exact expression (4.29) for the excess free-energy functional $\mathcal{F}_{\text{ex}}[\rho]$. We are free to choose the initial density $\rho_i(\mathbf{r})$ to be ρ_b , that of a uniform (bulk) reference fluid at the same chemical potential and temperature. Then $\Delta\rho(\mathbf{r}) = \rho(\mathbf{r}) - \rho_b$ and the grand potential functional becomes

$$\begin{aligned} \Omega_V[\rho] = \Omega[\rho_b] &+ \int d\mathbf{r} V(\mathbf{r})\rho(\mathbf{r}) + \beta^{-1} \int d\mathbf{r} \left[\rho(\mathbf{r}) \ln \frac{\rho(\mathbf{r})}{\rho_b} - \rho(\mathbf{r}) + \rho_b \right] \\ &+ \beta^{-1} \int_0^1 d\alpha (\alpha - 1) \int d\mathbf{r}_1 \int d\mathbf{r}_2 c^{(2)}([\rho_\alpha]; \mathbf{r}_1, \mathbf{r}_2) \Delta\rho(\mathbf{r}_1) \Delta\rho(\mathbf{r}_2), \end{aligned} \quad (5.3)$$

having used (4.17). Suppose now that we neglect the dependence of $c^{(2)}([\rho_\alpha]; \mathbf{r}_1, \mathbf{r}_2)$ on the coupling parameter α and, for simplicity, set this function equal to the two-body direct correlation function of the uniform reference fluid, so that:

$$c^{(2)}([\rho_\alpha]; \mathbf{r}_1, \mathbf{r}_2) \approx c^{(2)}(\rho_b; |\mathbf{r}_1 - \mathbf{r}_2|). \quad (5.4)$$

Then (5.3) simplifies to:

$$\begin{aligned} \Omega_V[\rho] = \Omega[\rho_b] &+ \int d\mathbf{r} V(\mathbf{r})\rho(\mathbf{r}) + \beta^{-1} \int d\mathbf{r} \left[\rho(\mathbf{r}) \ln \frac{\rho(\mathbf{r})}{\rho_b} - \rho(\mathbf{r}) + \rho_b \right] \\ &- (2\beta)^{-1} \int d\mathbf{r}_1 \int d\mathbf{r}_2 c^{(2)}(\rho_b; r_{12}) (\rho(\mathbf{r}_1) - \rho_b) (\rho(\mathbf{r}_2) - \rho_b). \end{aligned} \quad (5.5)$$

This functional can now be minimized, according to (4.11), and yields the following integral equation for the density profile:

$$\rho(\mathbf{r}_1) = \rho_b \exp[-\beta V(\mathbf{r}_1) + \int d\mathbf{r}_2 c^{(2)}(\rho_b; r_{12}) (\rho(\mathbf{r}_2) - \rho_b)], \quad (5.6)$$

which is the same as that obtained by making the HNC closure of the wall-particle Ornstein-Zernike equation. The wall-particle procedure treats the fluid as a homogeneous binary mixture of the particles or atoms, constituting the fluid of interest, and large spheres. One then takes the limit in which the density of the large spheres approaches

zero so the sphere acts as a structureless wall exerting an external potential $V(\mathbf{r})$. The Percus-Yevick (PY) version is a simple linearization of part of the exponent in (5.6), that is,

$$\rho(\mathbf{r}_1) = \rho_b \exp[-\beta V(\mathbf{r}_1)] \left[1 + \int d\mathbf{r}_2 c^{(2)}(\rho_b; r_{12})(\rho(\mathbf{r}_2) - \rho_b) \right]. \quad (5.7)$$

Both equations, along with closely related approximations based on alternative closures of the wall-particle Ornstein-Zernike equation, have been used in many studies of the density profile of liquids and gases near planar walls, where the sphere radius becomes infinite. While these theories are quite successful at describing the oscillatory profiles of hard spheres near planar hard walls, they are less successful when the fluid possesses an attractive, as well as a repulsive, component in the interatomic potential. One severe drawback of this type of theory is their inability to account for the presence of macroscopically thick wetting (or drying) films at a wall-fluid interface [30] or for the phenomenon of critical adsorption, which arises from the slow, algebraic decay of the density profile associated with the diverging bulk correlation length [31]. Such theories are not capable of describing phase transitions at fluid interfaces.

Their deficiencies can be best understood by reconsidering their generating functional (5.5). Clearly, this approximation retains only terms quadratic in the perturbation $\rho(\mathbf{r}) - \rho_b$; the logarithm merely reflects the ideal gas contribution. Note that $c^{(2)}(\rho_b; r)$ is fixed once μ and T are specified. If one considers (5.5) for bulk densities ρ , other than the initial ρ_b , one finds that the grand potential density

$$\omega(\rho) = \omega(\rho_b) + \beta^{-1} \left(\rho \ln \frac{\rho}{\rho_b} - \rho + \rho_b \right) - \frac{\beta^{-1}}{2} \int d\mathbf{r} c^{(2)}(\rho_b; r) (\rho - \rho_b)^2, \quad (5.8)$$

cannot account for liquid-gas coexistence [30]. A quadratic approximation is insufficient to describe two minima, which is a necessary requirement for coexistence in the uniform fluid. If the functional does not exhibit two minima (corresponding to bulk liquid and bulk gas), it cannot describe the development of a macroscopic wetting film, nor is it able to describe correctly the interface near the critical point, whose properties reflect (within the mean field approach) the coalescence of two minima [31].

It is straightforward to show that (5.5) is equivalent to retaining only the quadratic term in the functional Taylor expansion of $\mathcal{F}_{\text{ex}}[\rho]$ about the uniform reference value ρ_b . The next term in the expansion is

$$\frac{1}{3!} \int d\mathbf{r}_1 \int d\mathbf{r}_2 \int d\mathbf{r}_3 \left. \frac{\delta^3 \mathcal{F}_{\text{ex}}[\rho]}{\delta \rho(\mathbf{r}_1) \delta \rho(\mathbf{r}_2) \delta \rho(\mathbf{r}_3)} \right|_{\rho_b} (\rho(\mathbf{r}_1) - \rho_b)(\rho(\mathbf{r}_2) - \rho_b)(\rho(\mathbf{r}_3) - \rho_b),$$

where the functional derivative can be identified with $-\beta^{-1} c^{(3)}(\rho_b; \mathbf{r}_1, \mathbf{r}_2, \mathbf{r}_3)$, the three-body direct correlation function of the uniform fluid. Including such a term is sufficient to ensure that $\omega(\rho)$ does have two minima, so that coexistence and wetting are possible [32]. Applications and limitations of theories that include (approximately) the third-order term are reviewed briefly in Ref.[5].

Perhaps the best known application of the quadratic approximation (5.5) is in DFT treatments of the freezing transition in bulk liquids. In this context ρ_b in (5.5) refers to

the density of a uniform liquid and $\rho(\mathbf{r})$ to the average one-body density of the crystal; $V(\mathbf{r}) \equiv 0$. This approach to freezing was pioneered by Ramakrishnan and Yussouf [33, 34] and placed in the context of DFT by Haymet and Oxtoby [35]. We do not describe this work here as it will be covered in the lectures of Löwen. Rather we simply remark that, when considered as an approximate generating functional, (5.5) asserts,

$$c^{(2)}(\mathbf{r}_1, \mathbf{r}_2) = -\beta \frac{\delta^2 \mathcal{F}_{\text{ex}}[\rho]}{\delta \rho(\mathbf{r}_1) \delta \rho(\mathbf{r}_2)} = c^{(2)}(\rho_b; \mathbf{r}_{12}), \quad (5.9)$$

i.e. the pair direct correlation function of any inhomogeneous fluid, including the crystal, is equal to that of the bulk reference liquid. Clearly this constitutes a drastic assumption! That freezing does occur in this approximation (the free energy of the crystal with an imposed periodic density can be lower than that of the uniform liquid) for certain model systems might strike the reader as surprising, especially in the light of our remarks about the failure of this approximation to account for liquid-gas coexistence and wetting phenomena.

We conclude this subsection with a brief discussion of the structure of *bulk* fluids based on considerations that are similar to those above.

Consider a fluid with uniform density ρ_b , single out one atom, or test particle, and measure the positions of the remaining with respect to the center of that atom. Each of these atoms will experience an external potential that is identical to the interatomic pair potential $\phi(\mathbf{r}) \equiv \phi(r)$ exerted by the atom fixed at the origin. Percus [36] observed that the fluid then has a nonuniform density profile

$$\rho(\mathbf{r}) \equiv \rho(r) \equiv \rho_b g(r), \quad (5.10)$$

where $g(r)$ is the radial distribution function. It is clear that an approximate density functional theory, when applied to this particular type of inhomogeneity, will yield an approximation for $g(r)$; minimization of the approximate $\Omega_V[\rho]$, with $V(\mathbf{r}) = \phi(\mathbf{r})$, and solution of the resulting Euler-Lagrange equation is all that is required. Such a procedure yields standard integral equation theories of liquids and suggests new approximations.

The density profile can be expressed [see (4.16) and (4.17)] in the form

$$\rho(r) = \rho_b \exp[-\beta \phi(r) + c^{(1)}([\rho]; r) - c^{(1)}(\rho_b)], \quad (5.11)$$

which leads, via (5.10), to a self-consistency equation for the radial distribution function,

$$g(r) = \exp[-\beta \phi(r) + c^{(1)}([\rho_b g]; r) - c^{(1)}(\rho_b)]. \quad (5.12)$$

The exponent can be re-expressed, using (4.25) with $\rho_i = \rho_b$, as,

$$c^{(1)}([\rho]; r_1) - c^{(1)}(\rho_b) = \int_0^1 d\alpha \int d\mathbf{r}_2 (\rho(\mathbf{r}_2) - \rho_b) c^{(2)}([\rho_\alpha]; \mathbf{r}_1, \mathbf{r}_2),$$

so that (5.12) becomes

$$\ln g(r_1) = -\beta \phi(r_1) + \int_0^1 d\alpha \int d\mathbf{r}_2 \rho_b h(r_2) c^{(2)}([\rho_\alpha]; \mathbf{r}_1, \mathbf{r}_2), \quad (5.13)$$

where $h(r) \equiv g(r) - 1 = \rho(r)/\rho_b - 1$ is the total correlation function of the uniform fluid. Equation (5.13) is still exact but of no practical use until some approximation is made for $c^{(2)}([\rho_\alpha]; \mathbf{r}_1, \mathbf{r}_2)$, the quantity that refers to the nonuniform fluid of density $\rho_\alpha(\mathbf{r})$. The HNC approximation simply replaces this quantity by $c^{(2)}(\rho_b; r_{12})$, its value in the initial (bulk) state with $\alpha = 0$ [see (5.4)]. Thus the bulk HNC closure is

$$\ln g(r_1) = -\beta\phi(r_1) + \rho_b \int d\mathbf{r}_2 h(r_2) c^{(2)}(\rho_b; r_{12}). \quad (5.14)$$

Using the uniform fluid OZ equation, which follows from (4.20) with $\rho(\mathbf{r}) = \rho_b$,

$$h(r_1) = c^{(2)}(\rho_b; r_1) + \rho_b \int d\mathbf{r}_2 h(r_2) c^{(2)}(\rho_b; r_{12}), \quad (5.15)$$

(5.14) reduces to the familiar bulk HNC form

$$g(r) = \exp[-\beta\phi(r) + h(r) - c^{(2)}(\rho_b; r)]. \quad \text{HNC} \quad (5.16)$$

The bridge or elemental diagrams that are missing in the HNC can be reinstated formally via the inclusion of the bridge function $B(r)$:

$$g(r) = \exp[-\beta\phi(r) + h(r) - c^{(2)}(\rho_b; r) + B(r)]. \quad (5.17)$$

Approximate integral equation theories correspond to different prescriptions for $B(r)$ and some of the more sophisticated, modern versions yield results for both structure and thermodynamic functions that are in excellent agreement with simulation (e.g. [1] and [37]).

Comparison of (5.12) and (5.17) shows that $B(r)$ may be expressed as

$$B(r) = c^{(1)}([\rho_b g]; r) - c^{(1)}(\rho_b) - h(r) + c^{(2)}(\rho_b; r). \quad (5.18)$$

By expanding the first term about the density of the bulk fluid, we obtain

$$\begin{aligned} c^{(1)}([\rho_b g]; r_1) &= c^{(1)}(\rho_b) + \rho_b \int d\mathbf{r}_2 h(r_2) c^{(2)}(\rho_b; r_{12}) \\ &+ \sum_{n=2}^{\infty} \frac{\rho_b^n}{n!} \int d\mathbf{r}_2 \dots \int d\mathbf{r}_{n+1} h(r_2) \dots h(r_{n+1}) c^{(n+1)}(\rho_b; \mathbf{r}_1, \dots, \mathbf{r}_{n+1}). \end{aligned} \quad (5.19)$$

Use of the OZ equation (5.15) then leads to the exact expansion for the bridge function

$$B(r_1) = \sum_{n=2}^{\infty} \frac{\rho_b^n}{n!} \int d\mathbf{r}_2 \dots \int d\mathbf{r}_{n+1} h(r_2) \dots h(r_{n+1}) c^{(n+1)}(\rho_b; \mathbf{r}_1, \dots, \mathbf{r}_{n+1}), \quad (5.20)$$

in terms of the high-order direct correlation functions $c^{(n)}$ of the uniform fluid.

Truncation of (5.19) after the first order term, proportional to ρ_b , yields using (5.18) and (5.15), $B(r) = 0$, i.e. the HNC approximation (5.16). It is well-known [1] that the

HNC constitutes a reliable closure approximation for determining the structure of bulk fluids where the interatomic potential is long-ranged, e.g. in ionic fluids.

Approximations that go beyond HNC can be obtained by making assumptions about $c^{(3)}$ etc. entering (5.20). For example Barrat et. al. [38] used a real-space factorization ansatz for $c^{(3)}$ and neglected terms with $n > 2$ to construct an approximation for $B(r)$ and the resulting theory proved successful for soft spheres, the Lennard-Jones liquid and the OCP.

5.3 Approximations for Specific Model Fluids

In this subsection we describe approximate DFT's that have been developed for specific types of model fluid. In contrast to the interacting electron liquid where one seeks the universal exchange correlation function $E_{xc}[n]$, valid for all electronic materials, in classical DFT one often constructs an approximate functional $\mathcal{F}_{ex}[\rho]$ that is designed to treat a fluid of a particular type. The efficacy of a given DFT approximation can often be tested by making comparisons with computer simulation results.

We consider three different types of model fluid; these illustrate three very different approximate DFT's.

5.3.1 Hard-Sphere Fluids

Hard-sphere models play a vital role in the theory and simulation of liquids. At first site one might think that the properties of such systems would be rather dull. However, as mentioned in Section 2.2 even the single component hard-sphere model does something interesting. It is well-established from simulations that the model undergoes a first-order freezing transition to a fcc crystal at a reduced density $\rho_1\sigma^3 = 0.943$ and the crystal melts at $\rho_s\sigma^3 = 1.041$, where σ is the hard-sphere diameter. This purely entropy driven transition is described in the lectures by H. Löwen.

The binary hard-sphere mixture is defined by the pair potentials,

$$\phi_{ij}^{\text{hs}}(r) = \begin{cases} \infty; & r > \sigma_{ij}, \\ 0; & \text{otherwise,} \end{cases} \quad (5.21)$$

where $i, j = 1, 2$ label the species with diameter σ_{ij} . *Additive* mixtures are defined by $\sigma_{12} = (\sigma_{11} + \sigma_{22})/2$. These exhibit a plethora of different crystal structures; the phase diagram depends sensitively on the size ratio $q = \sigma_{22}/\sigma_{11}$. There is much discussion in the literature as to whether additive hard-sphere mixtures can exhibit fluid-fluid phase separation driven by so-called depletion attraction, i.e. whether the *effective* interaction between two large spheres (species 1) is sufficiently attractive at short separations, as a result of excluding the smaller species 2, to lead to two coexisting fluid phases. The present consensus from Monte Carlo simulations of the actual binary mixture and of studies of effective one-component models, is that fluid-fluid phase separation can occur for small size ratios $q \lesssim 0.1$ but this is always metastable with respect to the fluid-solid transition [39]. Strikingly for $q \lesssim 0.05$ there is a stable, isostructural solid-solid transition occurring at high densities of the large spheres.

One can also consider *non-additive* hard-sphere mixtures. These are defined by (5.21) but now $\sigma_{12} = (\sigma_{11} + \sigma_{22})(1 + \Delta)/2$ with the non-additivity parameter $\Delta \neq 0$. For positive non-additivity, $\Delta > 0$, the mixed state is disfavoured since the cross 12 interaction sets in at larger separations than the mean of the 11 and 22 interactions and stable fluid-fluid phase separation can occur in asymmetric mixtures with $q = 0.1$ [40]. An extreme non-additive mixture is the Asakura-Oosawa-Vrij (AO) model [41, 42, 43] of colloid-polymer mixtures in which the colloid-colloid interaction is hard-sphere like, with diameter σ_{cc} , and the colloid-polymer interaction is also hard-sphere like with diameter σ_{cp} , whereas the polymer-polymer interaction is zero, i.e. $\sigma_{pp} = 0$, corresponding to ideal interpenetrating coils. The cross-diameter $\sigma_{cp} = (\sigma_{cc} + 2R_g)/2$, where R_g is the radius of gyration of the polymer, so that $\Delta = 2R_g/\sigma_{cc}$. Approximate theories and simulation studies have shown that when the ratio $2R_g/\sigma_{cc}$ is $\gtrsim 0.35$ fluid-fluid phase separation is stable with respect to the fluid-solid transition, e.g. Refs. [44, 45].

DFT's have been developed for additive and non-additive hard-sphere mixtures. Most effort has focused on pure fluids and on the additive case. We do not attempt to review early work in any detail here. Since about 1980 there have been many attempts to develop weighted (or smoothed) density approximations. The general idea was to introduce a coarse-graining procedure whereby a smoothed density $\bar{\rho}(\mathbf{r})$ (or the set $\bar{\rho}_i(\mathbf{r})$ for the mixture) is constructed as an average of the true density profile $\rho(\mathbf{r})$ over a local volume. The pronounced peaks that occur in the oscillatory profile arising from the packing of the spheres, and where the local density may exceed that of close packing, are smoothed out in the coarse-grained $\bar{\rho}(\mathbf{r})$ so the excess free energy functional for a pure fluid should be well-represented by a *local* function of $\bar{\rho}(\mathbf{r})$:

$$F_{\text{ex}}^{\text{hs}}[\rho] = \int d\mathbf{r} \rho(\mathbf{r}) \psi_{\text{ex}}^{\text{hs}}(\bar{\rho}(\mathbf{r})), \quad (5.22)$$

where $\psi_{\text{ex}}^{\text{hs}}(\rho)$ is the excess, over ideal, free energy per hard-sphere. Different weighted density approximations (WDA) correspond to different recipes for constructing $\bar{\rho}(\mathbf{r})$ [5]. Note that (5.22) is similar in form to the exact result (4.34) for hard-rods. Some of these recipes are remarkably successful in accounting for the density profiles of hard-spheres adsorbed at walls or confined in slit pores; a summary is given in Ref. [5].

However, it is probably fair to argue that the FMT approach of Rosenfeld [20]; developed in 1989, has superseded the earlier approaches and is certainly the most widely-used theory (550 citations in ISI web of science as of August 2009). In these lectures we present a brief overview of FMT and some of its modifications and extensions.

Additive Mixtures: Rosenfeld Fundamental Measure Theory (FMT)

The original Rosenfeld theory was developed specifically for a ν component additive hard-sphere mixture in three dimensions $D = 3$ (Note that in this Section we use capital D for dimensionality rather than lower case d). It was motivated in part by the form of the exact excess free energy functional (4.34) for a hard-rod mixture in $D = 1$. The

other key ingredient is the exact low density limit:

$$\beta\mathcal{F}_{\text{ex}}[\{\rho_i\}] = -\frac{1}{2} \sum_{ij} \int d\mathbf{r} \int d\mathbf{r}' \rho_i(\mathbf{r}) \rho_j(\mathbf{r}') f_{ij}(|\mathbf{r} - \mathbf{r}'|), \quad (5.23)$$

valid for any fluid in the limit where all average one-body densities $\{\rho_i(\mathbf{r})\} \rightarrow 0$. The Mayer f function between particles of species i and j is

$$f_{ij}(r) = \exp(-\beta\phi_{ij}(r)) - 1, \quad (5.24)$$

where, as usual, $\phi_{ij}(r)$ is the pair potential between particles i and j . Equation (5.23) retains only the lowest-order term in a virial expansion of the functional. Taking the second functional derivative yields $c_{ij}^{(2)}(\mathbf{r}, \mathbf{r}') = f_{ij}(|\mathbf{r} - \mathbf{r}'|)$. The next term in the virial expansion contains the product of three Mayer bonds. For the particular case of hard spheres,

$$\begin{aligned} f_{ij}(r) &= \begin{cases} -1; & r < R_i + R_j, \\ 0; & \text{otherwise,} \end{cases} \\ &= -\theta(R_i + R_j - r), \end{aligned} \quad (5.25)$$

where R_i is the radius of species i , $i = 1, \dots, \nu$, and θ is the Heaviside (step) function. Rosenfeld [20] showed that these Mayer f functions can be decomposed as follows:

$$-f_{ij}(r) = \omega_i^{(3)} \otimes \omega_j^{(0)} + \omega_i^{(0)} \otimes \omega_j^{(3)} + \omega_i^{(2)} \otimes \omega_j^{(1)} + \omega_i^{(1)} \otimes \omega_j^{(2)} - \omega_i^{(2)} \otimes \omega_j^{(1)} - \omega_i^{(1)} \otimes \omega_j^{(2)}, \quad (5.26)$$

where the six weight functions are given by

$$\begin{aligned} \omega_i^{(3)}(\mathbf{r}) &= \theta(R_i - r), \\ \omega_i^{(2)}(\mathbf{r}) &= \delta(R_i - r); \quad \omega_i^{(2)}(\mathbf{r}) = \frac{\mathbf{r}}{r} \delta(R_i - r), \\ \omega_i^{(1)}(\mathbf{r}) &= \frac{\omega_i^{(2)}(\mathbf{r})}{4\pi R_i}; \quad \omega_i^{(1)}(\mathbf{r}) = \frac{\omega_i^{(2)}(\mathbf{r})}{4\pi R_i} \\ \omega_i^{(0)}(\mathbf{r}) &= \frac{\omega_i^{(2)}(\mathbf{r})}{4\pi R_i^2}, \end{aligned} \quad (5.27)$$

and the symbol \otimes denotes the 3 dimensional convolution of the weight functions:

$$\omega_i^{(\alpha)} \otimes \omega_j^{(\beta)}(\mathbf{r} = \mathbf{r}_i - \mathbf{r}_j) = \int d\mathbf{r}' \omega_i^{(\alpha)}(\mathbf{r}' - \mathbf{r}_i) \omega_j^{(\beta)}(\mathbf{r}' - \mathbf{r}_j). \quad (5.28)$$

For vector weights a scalar product is also implied.

The deconvolution (5.26) is of the same form as that of the Mayer f function for hard-rods in $D = 1$ where

$$-f_{ij}^{\text{hr}}(z) = \omega_i^{(1)} \otimes \omega_j^{(0)} + \omega_i^{(0)} \otimes \omega_j^{(1)}, \quad (5.29)$$

with the weight functions given by (4.36) and (4.37) and the convolution is the one-dimensional version of (5.28).

The weight functions (5.27) yield six weighted densities $\{n_\alpha(\mathbf{r})\}$ defined analogously to the one-dimensional case:

$$n_\alpha(\mathbf{r}) = \sum_{i=1}^{\nu} \int d\mathbf{r}' \rho_i(\mathbf{r}') \omega_i^{(\alpha)}(\mathbf{r} - \mathbf{r}'). \quad (5.30)$$

Now α labels four scalar and two vector weights. Note that for a uniform fluid of constant species density ρ_i both vector weighted densities \mathbf{n}_1 and \mathbf{n}_2 vanish and the scalar weighted densities reduce to the four scaled particle variables [46], i.e. $n_\alpha \rightarrow \xi^{(\alpha)}$, $\alpha = 0, 1, 2, 3$ where $\xi^{(3)} = \frac{4\pi}{3} \sum_i \rho_i R_i^3$, $\xi^{(2)} = 4\pi \sum_i \rho_i R_i^2$, $\xi^{(1)} = \sum_i \rho_i R_i$ and $\xi^{(0)} = \sum_i \rho_i$ and the summation is over all species. Clearly $\xi^{(3)}$ is the total packing fraction of the mixture. The $\{\omega_i^{(\alpha)}\}$ are characteristic functions of the sphere of radius R_i . This becomes clear on integrating each weight $w_i^{(\alpha)}$. For $\alpha = 3$ one obtains the volume $V_i = 4\pi R_i^3/3$; for $\alpha = 2$ the surface area $S_i = 4\pi R_i^2$; for $\alpha = 1$ the mean radius of curvature R_i ; and for $\alpha = 0$ the Euler characteristic which is simply 1. These are the *fundamental geometric measures* of the sphere of species i in three dimensions.

Following (4.34) for the exact one-dimensional case, Rosenfeld made the following ansatz for the excess free energy functional of the hard-sphere mixture:

$$\beta \mathcal{F}_{\text{ex}}[\{\rho_i\}] = \int d\mathbf{r} \Phi(\{n_\alpha(\mathbf{r})\}), \quad (5.31)$$

where $\beta^{-1}\Phi$, the excess free energy density is a *function* of the weighted densities. Further he assumed that

$$\Phi(\{n_\alpha\}) = f_1(n_3)n_0 + f_2(n_3)n_1n_2 + f_3(n_3)\mathbf{n}_1 \cdot \mathbf{n}_2 + f_4(n_3)n_2^3 + f_5(n_3)n_2\mathbf{n}_2 \cdot \mathbf{n}_2, \quad (5.32)$$

where the coefficients f_α depend only on n_3 . Each term in (5.32) has dimension $[\text{length}]^{-3}$; this form is motivated by dimensional analysis.

Eqns. (5.31) and (5.32) must recover the exact low density limit (5.23) and this demands that to lowest order in n_3 the f_α must have expansions $f_1 = n_3 + O(n_3^2)$, $f_2 = 1 + O(n_3)$, $f_3 = -1 + O(n_3)$, $f_4 = 1/24\pi + O(n_3)$, and $f_5 = -3/24\pi + O(n_3)$.

For intermediate and high densities it is necessary to impose additional physical requirements in order to determine the coefficients f_α . Rosenfeld invoked the requirement:

$$\lim_{R_i \rightarrow \infty} \left(\frac{\mu_{\text{ex}}^i}{V_i} \right) = p, \quad (5.33)$$

where $V_i \equiv 4\pi R_i^3/3$ is the volume of sphere i . This result simply states that the excess chemical potential for inserting a hard-sphere of species i into a uniform fluid at pressure p is pV_i plus a contribution proportional to the surface area. μ_{ex}^i is given by

$$\beta \mu_{\text{ex}}^i = \frac{\partial \Phi}{\partial \rho_i} = \sum_{\alpha} \frac{\partial \Phi}{\partial n_{\alpha}} \frac{\partial n_{\alpha}}{\partial \rho_i}, \quad (5.34)$$

and from the definition of the scaled particle variables (recall $n_\alpha = \xi^{(\alpha)}$ for the uniform fluid) $\partial n_3/\partial \rho_i = 4\pi R_i^3/3$, $\partial n_2/\partial \rho_i = 4\pi R_i^2$, $\partial n_1/\partial \rho_i = R_i$ and $\partial n_0/\partial \rho_i = 1$. Thus

$$\lim_{R_i \rightarrow \infty} \left(\frac{\beta \mu_{\text{ex}}^i}{V_i} \right) = \frac{\partial \Phi}{\partial n_3}. \quad (5.35)$$

The pressure is obtained from the thermodynamic relation $\Omega_b = -pV$, valid for a bulk fluid, with the grand potential density given by $\Omega_b/V = \beta^{-1}\Phi + f_{\text{id}} - \sum_i \rho_i \mu_i$. Combining these results and using (5.33) one obtains the scaled particle differential equation,

$$\frac{\partial \Phi}{\partial n_3} = -\Phi + \sum_\alpha \frac{\partial \Phi}{\partial n_\alpha} n_\alpha + n_0. \quad (5.36)$$

Rosenfeld solved this equation for the five coefficients f_α ; integration constants are chosen so that the correct low density limits are recovered. The solution is

$$\begin{aligned} f_1(n_3) &= -\ln(1 - n_3); & f_2(n_3) &= (1 - n_3)^{-1}; & f_3(n_3) &= -f_2(n_3); \\ f_4(n_3) &= [24\pi(1 - n_3)^3]^{-1}; & f_5(n_3) &= -3f_4(n_3). \end{aligned} \quad (5.37)$$

Note that the conditions $f_3 = -f_2$ and $f_5 = -3f_4$, that determine the contributions of vector weighted densities to the functional, follow by assuming that the differential equation constructed for a uniform fluid remains valid in slightly inhomogeneous situations. Recall that the vector weighted densities vanish in the limit of a uniform fluid.

The resulting functional is usually written as

$$\Phi = \Phi_1 + \Phi_2 + \Phi_3, \quad (5.38)$$

with

$$\Phi_1 = -n_0 \ln(1 - n_3); \quad \Phi_2 = \frac{n_1 n_2 - \mathbf{n}_1 \cdot \mathbf{n}_2}{1 - n_3}, \quad (5.39)$$

and

$$\Phi_3 = \frac{n_2^3 - 3n_2 \mathbf{n}_2 \cdot \mathbf{n}_2}{24\pi(1 - n_3)^2}. \quad (5.40)$$

In the limit of a uniform fluid Φ is identical to the Percus-Yevick (compressibility) excess free energy density of the hard-sphere mixture, expressed in scaled particle variables. This is known to yield a reasonably accurate equation of state for a large range of total density, provided the mixture is not very asymmetric.

The functional (5.31) generates a hierarchy of direct correlation functions $c_{i_1, \dots, i_m}^{(m)}$ that have a very simple structure,

$$\begin{aligned} c_{i_1, \dots, i_m}^{(m)}(\mathbf{r}_1, \dots, \mathbf{r}_m) &= -\beta \frac{\delta^m \mathcal{F}_{\text{ex}}[\{\rho_i\}]}{\delta \rho_{i_1}(\mathbf{r}_1) \dots \delta \rho_{i_m}(\mathbf{r}_m)} \\ &= -\int d\mathbf{r} \sum_{\alpha_1, \dots, \alpha_m} \frac{\partial^m \Phi}{\partial n_{\alpha_1} \dots \partial n_{\alpha_m}} \omega_{i_1}^{(\alpha_1)}(\mathbf{r}_1 - \mathbf{r}) \dots \omega_{i_m}^{(\alpha_m)}(\mathbf{r}_m - \mathbf{r}). \end{aligned} \quad (5.41)$$

Once again a scalar product is implied for vector weights. In the uniform fluid, where the weighted densities are independent of position, the form is particularly simple. For example, the pair function ($m = 2$) has the Fourier transform:

$$c_{ij}^{(2)}(k) = - \sum_{\alpha, \beta} \frac{\partial^2 \Phi}{\partial n_\alpha \partial n_\beta} \omega_i^{(\alpha)}(k) \omega_j^{(\beta)}(k), \quad (5.42)$$

where k is the wave number.

It turns out that these pair direct correlation functions $c_{ij}^{(2)}$ are identical to those from the Percus-Yevick (PY) theory of the uniform mixture. The PY theory provides a good description of the pair correlation functions of hard-sphere mixtures for moderate total densities and asymmetries that are not too extreme.

It is remarkable that the geometrically-based approach of Rosenfeld leads to a functional that *generates* both the free energy density and the pair correlation functions of the uniform hard-sphere *mixture* treated in PY approximation. Insightful connection is made with scaled-particle theory, [46] and although several heuristic assumptions are made in the derivation, Rosenfeld's construction of the FMT was a major step forward in DFT treatments of inhomogeneous hard-particle systems. The mixture aspect is important; earlier weighted density approximations struggled to treat multi-component systems [5].

Shortly after Rosenfeld published his paper, Kierlik and Rosinberg [47] presented an alternative version of the DFT that employs four scalar weight functions and no vector weights. Two weights are the same as $\omega_i^{(2)}$ and $\omega_i^{(3)}$ of (5.27). The other two involve derivatives of delta functions. By *requiring* their functional to generate the PY results for $c_{ij}^{(2)}$ and the excess free energy density, Kierlik and Rosinberg derived a DFT that appeared to be different from that of Rosenfeld. Subsequently it was shown [48] that the two versions are equivalent; they will yield the same density profiles and free energies for any external potential. The de-convolution of the Mayer f -function is not unique; the two versions correspond to different de-convolutions.

There have been many applications of the Rosenfeld (or Kierlik-Rosinberg) FMT for different types of confinement. These include the pure hard-sphere fluid adsorbed at a single planar wall [47], and mixtures adsorbed at walls or in model pores [49, 50]. The agreement between the results of the FMT and those of computer simulation for density profiles is generally very good; the functional captures the effects of short-ranged correlations, i.e. the packing of the spheres that gives rise to strongly oscillatory profiles. The FMT also captures selectivity effects arising from the difference in size between the species.

One noteworthy shortcoming of the original Rosenfeld FMT is that it fails to account for the freezing transition of the pure hard-sphere fluid [20, 47, 49, 50]. Crystallization can be viewed as a particular type of strong confinement whereby particles remain localized near their (perfect) lattice sites, undergoing excursions with a small root-mean square deviation. Considerations of particular classes of confinement led to subsequent extensions of the theory and we summarize some of these below. A comprehensive re-

view of the development and extensions of FMT is given in the excellent recent review by Tarazona et.al. [50]. There is also an illuminating new review by Roth [51].

Extensions and Modifications of the Rosenfeld Functional

Rosenfeld et. al. [52] invoked the notion of *dimensional crossover*, examined in earlier weighted density approaches [53], to propose modifications to the FMT. The basic idea is that a DFT constructed for a three dimensional inhomogeneous fluid should remain an accurate approximation for lower effective dimensionality D , e.g. for the fluid confined to very narrow slits (2D), or narrow cylinders (1D) or even cavities that cannot hold more than one particle (0D).

For a pure fluid in the 2D *limit* the imposed distribution is $\rho(\mathbf{r}) = \rho_{2D}(x, y)\delta(z)$, i.e. a delta function along the z -axis, and the original Rosenfeld FMT with excess free energy density given by (5.38-5.40) provides a reasonably accurate free energy density.

In the 1D *limit* where $\rho(\mathbf{r}) = \rho_{1D}(x)\delta(y)\delta(z)$ the dimensional reduction fails since the term Φ_3 given by (5.40) yields non-integrable singularities. However, the sum $\Phi_1 + \Phi_2$ yields the exact result for the excess free energy density Φ^{hr} (4.38) in one-dimension.

The strict 0D *limit* sets $\rho(\mathbf{r}) = \eta_0\delta(x)\delta(y)\delta(z)$ where $\eta_0 \leq 1$ is the mean number of particles in the small cavity. Tarazona and Rosenfeld [54] considered the case of a cavity that cannot hold more than one hard-sphere and showed that provided the distance between any two points with $\rho(\mathbf{r}) \neq 0$ is $< \sigma$, the hard-sphere diameter, the excess free energy functional can be calculated exactly for any allowed distribution $\rho(\mathbf{r})$. They find

$$\beta\mathcal{F}_{\text{ex}}^{\text{0D}} = \phi_0 = (1 - \eta_0) \ln(1 - \eta_0) + \eta_0, \quad (5.43)$$

which depends upon $\rho(\mathbf{r})$ via only its total integral $\eta_0 = \int d\mathbf{r}\rho(\mathbf{r})$.

Demanding that a DFT constructed for three dimensions should reproduce the exact free-energy (5.43) for a 0D cavity is clearly a stringent requirement. In Ref. [52] Rosenfeld et. al. proposed empirical modifications to Φ_3 in the original FMT that yield an accurate approximation to the 0D free-energy but also retain a good description of the 3D hard-sphere fluid, i.e. the Percus-Yevick free-energy density and pair direct correlation functions. Moreover, the modifications provided a rather good description of hard-sphere freezing. Subsequently Gonzalez et. al. [55] showed that the modified versions performed better than the original FMT in accounting for the results of Monte Carlo simulations of the density profile $\rho(r)$ of the hard-sphere fluid confined in a spherical (hard) cavity, especially for situations where packing constraints lead to a pronounced peak in $\rho(r)$ in the centre of the cavity.

Tarazona and Rosenfeld [54] developed a new strategy for constructing $\mathcal{F}_{\text{ex}}[\rho]$ in 3D based only on the requirement that the exact 0D limit is recovered over a partial set of cavity shapes. The building blocks are the local packing fraction $n_3(\mathbf{r})$ and density convolutions with spherical δ shells of radius R . Spurious divergences can be eliminated and it is argued that the free energy of the 3D uniform hard-sphere fluid is an output of the theory given in terms of successive derivatives of the 0D excess free energy ϕ_0 in (5.43). There are classes of cavity shapes, termed lost cases, for which the set of one-centre convolution weight functions used in the original FMT are inadequate. This led

Tarazona [56] to introduce a dimensional interpolation version of FMT that is designed to recover the Percus-Yevick $c^{(2)}(r)$ and compressibility equation of state for the uniform fluid, as in FMT, but uses the elements of Ref. [54] to eliminate the spurious divergences in the 1D limit and recover the exact 0D limit. The resulting functional has the same form as FMT but with Φ_3 replaced by Φ_3^T that depends on a rank-2 tensor density $T(\mathbf{r})$. Neglecting the anisotropy of $T(\mathbf{r})$ but retaining its trace: $\text{tr}[T] = n_0(\mathbf{r})$, one recovers the original FMT. Retaining the anisotropy ensures the cancellation of the spurious divergence of Φ_3 in the 1D limit. Tarazona's dimensional interpolation version provides a remarkably accurate account of the properties of the hard-sphere crystal [56]. In fact the predicted equation of state is more accurate than the Percus-Yevick compressibility approximation is for the high-density fluid!

It turns out that extending the dimensional interpolation procedure to additive hard-sphere mixtures is not straightforward. The direct analogue, somewhat surprisingly, does not recover the exact 1D limit although the one-component case does and a new rank-3 tensor weighted density must be introduced to correct for this [57]. However, the two versions yield essentially the same results for a binary mixture, with size ratio 5, adsorbed at a planar hard wall or in a narrow slit pore suggesting that the simpler to implement dimensional interpolation version should be sufficient for most purposes [57, 50].

Whilst it is appealing to build DFTs on the basis of the 0D limit, there is, of course, nothing sacrosanct about this. Pragmatically one seeks a DFT that performs accurately for a wide range of inhomogeneities; it is a bonus if the theory happens to be based on an elegant prescription! One such pragmatic approach to improving the one-component FMT was made by Tarazona [58]. This maintains the dimensional interpolation (tensor) structure but adjusts Φ_3 so that in the fluid phase the very accurate Carnahan-Starling (CS) equation of state is recovered.

Roth et. al. [59] introduced the so called White Bear version that employs the accurate Mansoori-Carnahan-Starling-Leland (MCSL) bulk equation of state for binary mixtures as *input* to the theory. Roth et. al. solved (5.36) but with the l.h.s. replaced by the pressure βp_{MCSL} . The coefficients f_α are then re-calculated and one finds f_1 and f_2 unchanged from the original FMT, but f_4 is modified. The conditions $f_3(n_3) = -f_2(n_3)$ and $f_5(n_3) = -3f_4(n_3)$ are retained. The upshot is that Φ_3 in (5.40) is replaced by

$$\Phi_3^{\text{WB}} = (n_2^3 - 3n_2\mathbf{n}_2 \cdot \mathbf{n}_2) \frac{n_3 + (1 - n_3)^2 \ln(1 - n_3)}{36\pi n_3^2 (1 - n_3)^2}. \quad (5.44)$$

In the limit $n_3 \rightarrow 0$, $f_4(n_3) \rightarrow 1/(24\pi)$ and the exact low-density limit of the functional is recovered. Note that the same free energy density was proposed earlier [47] but not implemented. The White-Bear functional faces similar problems to those encountered in the original FMT when applied to the freezing transition or in the 1D or 0D limits. For a one-component fluid Roth et.al. [59] proposed replacing the term $(n_2^3 - 3n_2\mathbf{n}_2 \cdot \mathbf{n}_2)$ by the term that enters Tarazona's [56] tensor version of Φ_3 . The resulting theory is identical to that in [58] and improves the values calculated for coexisting liquid and crystal densities: $\rho_l \sigma^3 = 0.934$ and $\rho_s \sigma^3 = 1.023$. These should be contrasted with the results of Tarazona's dimensional interpolation theory, which retains the Percus-Yevick

equation of state for the fluid and yields $\rho_l\sigma^3 = 0.892$ and $\rho_s\sigma^3 = 0.985$ [58].

The White Bear version generates pair direct correlation functions, via (5.41), that have the same *form* as those from the original FMT which, recall, are those of Percus-Yevick theory. Since the weight functions are the same as those used in FMT the $c_{ij}^{(2)}(r)$ of the uniform fluid also vanish for $r > R_i + R_j$ [59]. In the one-component case $c^{(2)}(r)$ calculated from the White Bear version is in better agreement with simulation results for $\rho\sigma^3 = 0.8$ than is the Percus-Yevick result [59]. Roth et. al. [59] calculated density profiles for hard-sphere fluids adsorbed at planar walls. In general the results from the White Bear version lie very close to those from the Rosenfeld FMT apart from distances very close to the wall. Density functional theories that are based on weighted density approximations satisfy the exact hard wall contact theorem, i.e. $\sum_i \rho_{w_i} = \beta p$, where p is pressure of the bulk fluid far from the wall and ρ_{w_i} is the local density of species i in contact with the wall. Since the White Bear version is constructed to yield the accurate MCSL equation of state for the mixture (and CS for the one component fluid) it is guaranteed to yield results closer to those of simulation than the original FMT for distances that are close to contact but not necessarily at larger distances.

Independently of Ref. [59], Yu and Wu [60] developed the same extension of the theory. Of course, they did not call it the White Bear version. In a subsequent paper Yu et.al. [61] applied the theory to study size selectivity in *polydisperse* hard-sphere mixtures adsorbed at a hard wall. The results agree well with simulation, even better than those of Pagonabarraga et. al. [62] who used the original Rosenfeld FMT. These applications to polydisperse systems are important in illustrating the power of the FMT approach for mixtures. As emphasized earlier, WDA's are not easily extended to mixtures [5] whereas Rosenfeld's FMT is a theory designed specifically for mixtures. It would not be feasible to tackle problems of polydispersity using WDA's where the weight functions depend on the local densities. Another interesting application of FMT, with the empirical modifications of Ref. [52], was made in the study of entropic selectivity of hard-sphere mixtures confined in model nano-pores [63].

We conclude this brief discussion of extensions of the Rosenfeld functional by returning to an issue of self-consistency. Recall that in the derivation of the original Rosenfeld functional the relation $\beta p = \partial\Phi/\partial n_3$ is *imposed*-see (5.33)-(5.35). The pressure p obtained by solving (5.36) is the scaled particle or Percus-Yevick compressibility result. Within the White Bear version the above relation is not imposed and one can enquire how the pressure calculated from this relation differs from p_{MCSL} that is input into the theory. This was addressed in Ref. [59] for a one-component fluid. Remarkably the pressure given by $\beta^{-1}\partial\Phi/\partial n_3$ differs by at most 2% from the accurate p_{CS} for densities up to freezing which attests to the high degree of self-consistency. In contrast the Percus-Yevick compressibility result overestimates the pressure close to freezing by about 7%. In later papers Hansen-Goos and Roth [64, 65] proposed a new generalization of the Carnahan-Starling equation of state to mixtures that is somewhat more accurate than the MCSL version and derived an excess free energy functional following the White Bear route. This White Bear Mark II version is constructed so that in the one-component fluid $\partial\Phi/\partial n_3 = \beta p_{\text{CS}}$. It was applied successfully to the calculation of the surface ten-

sion and other interfacial coefficients for a hard-sphere fluid adsorbed at a hard spherical surface [65]. The review by Roth [51] provides a summary of recent developments and applications, comparisons between different versions of FMT and gives a valuable guide to the practical implementation of FMT.

Non-Additive Mixtures

So far we have considered functionals constructed for additive hard-sphere mixtures. In recent years there has been much progress in designing functionals that will treat specific non-additive models. This is a rapidly growing topic and we cannot do justice to it in the present lecture notes. We refer the reader to the review [50] (see Section 7.9) for a useful overview and to the articles of Schmidt [66] and Brader et.al. [67] for summaries of developments up to 2003. The last article focuses on models for colloid-polymer mixtures.

From the outset one should note that non-additive mixtures are considerably more difficult to treat than additive ones; even in $D = 1$ the exact free-energy functional is not known for any non-additive case. Here we mention a few cases where geometry-based DFT's have been constructed and applied.

The *Asakura-Oosawa-Vrij (AO)* model of colloid-polymer mixtures has been well-studied using a variety of statistical mechanical techniques [67]. Schmidt et.al. [68, 69] devised a DFT specifically for this model following the FMT scheme and the 0D treatment of Ref. [54]. For the AO model the 0D cavity can hold at most one hard-sphere colloid but can hold an arbitrary number of ideal polymers if no colloid is present. The 0D excess free energy can be calculated exactly and differs from that in (5.43). The resulting functional has several appealing features:

- i) for a uniform fluid mixture it yields a bulk free energy density that is identical to that from the free-volume theory of Lekkerkerker et. al. [70] that is known to provide a reasonable account of fluid phase equilibria in the AO model.
- ii) by construction it satisfies the correct 0D limit.
- iii) it generates, via the test particle route, the correct depletion potential between two hard-sphere colloids immersed in the sea of ideal polymer.
- iv) the bulk pair direct correlation functions $c_{ij}^{(2)}(r)$ are given analytically so that the partial structure factors $S_{ij}(k)$ are given explicitly and the results are in quite good agreement with those from simulation [69].
- v) the theory is linear in the polymer density $\rho_p(\mathbf{r})$. This ensures $c_{pp}^{(2)}(r) = 0$, as in Percus-Yevick approximation, and it also means that $\rho_p(\mathbf{r})$ can be obtained explicitly as a functional of the colloid density $\rho_c(\mathbf{r})$, simplifying the minimization procedure.

On the negative side the functional does not yield the correct 1D limit. This could be corrected [50].

Schmidt et.al. [71] attempted to incorporate polymer-polymer repulsion by introducing a repulsive step-function pair potential $\phi_{pp}(r) = \epsilon$, $r < 2R_g$ and 0 otherwise. The resulting DFT captures several, but not all of the effects of polymer-polymer excluded volume interactions that are found in computer simulations of bulk phase behaviour which employ realistic effective potentials for polymer-polymer interactions [45].

There have been many applications of the DFT for the AO model to inhomogeneous colloid-polymer mixtures [67]. These include studies of the 'free' interface between colloid-rich (liquid) and colloid-poor (gas) fluid phases and adsorption phenomena at the interface between the AO mixture and a hard wall. For size ratios $2R_g/\sigma_{cc}$ between 0.6 and 1.0 rich behaviour is found. For example, oscillatory density profiles are predicted for the free interface and novel wetting and layering transitions are predicted for the hard wall-colloid gas interface. The DFT studies motivated computer simulations by Dijkstra and van Roij [72] who found jumps in the adsorption which they attributed to layering transitions of the type determined in the DFT calculations of Brader et.al. As emphasized in Ref. [67] there are important differences between the type of layering (and wetting) transitions found in the AO model and those found in DFT and simulation studies of the adsorption of simple gases at strongly attractive substrates. In the latter case layering always occurs close to the bulk triple point where the density profiles are highly structured and the individual fluid layers appear very pronounced. By contrast, in the AO model layering transitions can occur at state points well-removed from the triple point and the colloid density profiles are not as highly structured.

Other applications of the AO functional are a) to capillary condensation of the AO mixture confined by two parallel planar hard walls where depletion attraction favours condensation of the colloid-rich (liquid) phase [73], b) to the mixture exposed to a standing laser field modelled as an external potential acting on the colloids that can stabilize a 'stacked' fluid phase consisting of a periodic succession of liquid and gas slabs [74], and c) to sedimentation equilibria where a novel floating liquid phase was found [75].

Another model for which a DFT has been constructed is the *Widom-Rowlinson* model [76]. This is a ν -component non-additive hard-sphere mixture of radii R_i where the mixing rule is such that particles of like species are non-interacting while unlike species exhibit infinite repulsion for separation $r < R_i + R_j$ and 0, otherwise. This choice favours fluid-fluid demixing. Schmidt [77] followed the same procedure as for the AO model, calculating the excess free energy for the 0D cavity and taking derivatives of this w.r.t. the packing fraction to obtain the quantities entering the free energy density Φ . The resulting theory provides a reasonably successful description of the radial distribution functions $g_{ij}(r)$ and of fluid-fluid demixing in the uniform binary model, $\nu = 2$. Two phase coexistence occurs at high total density and the DFT underestimates the critical density from simulation by about 30%. Nevertheless this value is somewhat better than from other mean-field treatments [77].

Perhaps the most ambitious development is that of Schmidt [78] who has introduced a DFT, based on FMT ideas, for a *general class of non-additive hard-sphere mixtures*. The jury is out regarding how accurate Schmidt's functional is when tested against

simulation.

We do not discuss DFT's for fluids composed of hard *anisotropic* particles as this takes us into the realm of Löwen's lectures. Rather we alert the reader to the summary in Sections 7.10 and 7.11 of Ref. [50]. Using a hard potential to model real molecules that exhibit liquid crystalline phases is often a gross over-simplification. However, for colloid liquid crystals this is a reasonable first approximation. The Letter by Hansen-Goos and Mecke [79] represents the state-of-the-art in recent development of FMT for anisotropic fluids.

5.3.2 The Lennard-Jones (LJ) Type Fluid

How does one devise a DFT for a fluid or a fluid mixture, in which the particles interact via a pair potential which has both a sharply repulsive piece, dominant at small separations r , and a longer ranged attractive piece dominating at large r ? Such pair potentials are directly relevant to simple fluids, e.g. the noble gases, and their mixtures. It is for such systems that one might expect DFT to be most advanced.

In reality there is little progress in treating attractive interactions within DFT. Most treatments begin by approximating the free energy functional arising from repulsive interactions by that of a hard sphere system with appropriately chosen hard-sphere diameters. How one chooses the latter is a matter for discussion but the well-known Barker-Henderson prescription [1] has the merit of yielding density independent effective hard sphere diameters. Attractive interactions are usually treated within a mean-field approximation, i.e. correlations are neglected in this part of the functional. For a mixture of LJ fluids the standard ansatz for the excess free energy functional is

$$\mathcal{F}_{\text{ex}}[\{\rho_i\}] = \mathcal{F}_{\text{ex}}^{\text{hs}}[\{\rho_i\}] + \frac{1}{2} \sum_{i,j} \int d\mathbf{r} \int d\mathbf{r}' \rho_i(\mathbf{r}) \rho_j(\mathbf{r}') \phi_{ij}^{\text{att}}(\mathbf{r} - \mathbf{r}'), \quad (5.45)$$

where $\mathcal{F}_{\text{ex}}^{\text{hs}}$ is the excess free energy functional of the hard-sphere mixture, with appropriately chosen diameters. $\mathcal{F}_{\text{ex}}^{\text{hs}}$ is obtained from FMT or one of the earlier weighted-density approximations. $\phi_{ij}^{\text{att}}(r)$ is the attractive part of the pair potential between species i and j .

One can motivate (5.45) in several ways. Formally one can write the free energy functional as that of a suitable repulsive reference fluid at the same temperature and density distributions $\{\rho_i(\mathbf{r})\}$ plus a contribution that incorporates the attractive perturbation—see eg. (33) in Ref. [5]. By making a crude mean-field approximation in this contribution and approximating the free energy functional of the reference system by that of a hard sphere fluid one arrives at (5.45). Note that for a homogeneous binary fluid mixture (5.45) yields

$$f_{\text{ex}}(\rho_1, \rho_2) = f_{\text{ex}}^{\text{hs}}(\rho_1, \rho_2) - \frac{1}{2} \sum_{i,j} \rho_i \rho_j a_{ij}, \quad (5.46)$$

for the excess free energy density of a mixture with constant densities ρ_1 and ρ_2 . Here $a_{ij} = - \int d\mathbf{r} \phi_{ij}^{\text{att}}(r)$ is the integrated strength of the attractive potential between i and

j. Clearly (5.46) provides a van der Waals-like approximation for the free energy of the bulk mixture [1, 5]. Perhaps the best way to understand the approximation (5.45) is to take two functional derivatives:

$$c_{ij}^{(2)}(\mathbf{r}_1, \mathbf{r}_2) = -\beta \frac{\delta^2 \mathcal{F}_{\text{ex}}[\{\rho_i\}]}{\delta \rho_i(\mathbf{r}_1) \delta \rho_j(\mathbf{r}_2)} = c_{ij}^{\text{hs}}(\mathbf{r}_1, \mathbf{r}_2) - \beta \phi_{ij}^{\text{att}}(r_{12}), \quad (5.47)$$

i.e. the pair direct correlation function is that of the inhomogeneous hard-sphere mixture reference fluid c_{ij}^{hs} plus a term proportional to the attractive pair potential. In the limit of a homogeneous fluid (5.47) reduces to

$$c_{ij}^{(2)}(r_{12}) = c_{ij}^{\text{hs}}(r_{12}) - \beta \phi_{ij}^{\text{att}}(r_{12}), \quad (5.48)$$

where the density dependence in the hard-sphere term has not been made explicit. Equation (5.48) is often referred to as a random phase approximation (RPA) for treating attractive pair potentials [1]. It has the advantage of capturing i) short-ranged correlations arising from repulsive forces between the particles (packing effects) and ii) the correct asymptotic decay of correlations, i.e. $c_{ij}^{(2)}(r) \approx -\beta \phi_{ij}(r)$, as $r \rightarrow \infty$. However, the RPA treatment provides a poor quantitative account of the radial distribution functions $g_{ij}(r)$, obtained from the mixture generalization of the OZ equation (5.15), at separations r corresponding to contact. In particular the RPA can yield negative values of $g_{ij}(r)$ inside the hard-core. Moreover the results are dependent upon how the attractive perturbation $\phi_{ij}^{\text{att}}(r)$ is defined inside the core.

Nevertheless, (5.45) remains the work-horse functional for studies of interfacial problems and effects of confinement in simple fluids and their mixtures. It has several advantages over the generic approximations discussed in Section 5.2. The main ones are: i) dispersion forces are incorporated, i.e. the algebraic decay of the pair potentials is treated properly and ii) it is straightforward to prove that the DFT is thermodynamically consistent, i.e. the resulting density profiles and adsorption are consistent with the Gibbs adsorption equation and the profiles satisfy certain exact sum rules, including the hard wall contact theorem mentioned earlier. Thermodynamic consistency is a key requirement for a DFT since one of the main applications is in studying phase equilibria in inhomogeneous systems. Results should not depend on which route is employed to calculate the adsorption. The main disadvantages of (5.45) lie in its mean-field character. It is clear from the result (5.46) for the free energy density of the bulk fluid that the theory will yield van der Waals (mean-field) critical exponents. The RPA treatment of the attractive potential does not incorporate the effects of bulk critical fluctuations. In keeping with other DFTs (5.45) also omits the capillary wave fluctuation-induced broadening of the density profiles at fluid-fluid interfaces in weak external fields.

In spite of these shortcomings, this DFT approximation has found an enormous number of applications, especially for one-component fluids. Some of these are reviewed in Ref. [5]. We do not attempt to provide a comprehensive account of the many applications. Rather we refer the reader to recent papers concerned with the wetting by gas of a square-well [80] and a Lennard-Jones type liquid [81, 82] adsorbed at a spherical substrate. These papers illustrate how a DFT that is thermodynamically consistent can

be used to investigate quantitatively a large variety of interfacial phenomena, including the subtle behaviour associated with curvature of the substrate. The case of dispersion forces, equation (2.1), is especially important since in this case a mean-field DFT captures the correct critical exponents that describe the divergence of the thickness of a wetting film and the correlation length of density fluctuations parallel to the (planar) substrate. The technical reason underlying this bonus for DFT is that the upper critical dimension for both complete and critical wetting in systems with power-law potentials is < 3 [83].

There have been attempts to improve upon the mean-field treatment of attractive interactions. Intuitively one expects the integrand in the second term of (5.45) to include a factor that accounts for the pair correlations of the reference fluid. The formal treatment outlined in Ref. [5] gives the full expression but this cannot be implemented without making several approximations. One approach, for a pure fluid, is to insert a factor $g^{\text{hs}}(\bar{\rho}; |\mathbf{r} - \mathbf{r}'|)$, where the radial distribution function of the hard sphere fluid is evaluated at some average or weighted density $\bar{\rho}$ that depends on the local density at \mathbf{r} and \mathbf{r}' . The theory becomes considerably more complicated to implement since functional differentiation of $g^{\text{hs}}(\bar{\rho}; |\mathbf{r} - \mathbf{r}'|)$ is involved [84].

An interesting alternative approach for incorporating attractive interactions into a FMT has been developed by Lutsko [85]. Oettel [86] has developed a general reference functional approach. Both approaches seem rather promising.

5.3.3 Soft Core Model Fluids: the RPA Functional

There is a rapidly growing literature on the properties of soft core (penetrable) model fluids. Much of the motivation for considering such models comes from polymer physics where blob models describe the effective interaction between the centres of mass of polymer coils. For example, the Gaussian core model (GCM) defined by

$$\phi(r) = \epsilon \exp(-r^2/R^2), \quad (5.49)$$

where the energy scale $\epsilon > 0$ and the range R is roughly the radius of gyration of the polymer, provides a reasonably accurate description of the effective interaction between two identical polymer coils in an athermal solvent provided $\epsilon \sim \text{few } k_{\text{B}}T$. Indeed the Gaussian shape remains a good approximation to the effective potential in dilute and semidilute solutions of self-avoiding random walk (SAW) polymers and the parameter ϵ does not vary strongly with the concentration: $\epsilon \approx 2k_{\text{B}}T$ [87]. The GCM reproduces the structure and thermodynamic properties of SAW polymer solutions over a wide concentration range [87]. Such a procedure of integrating out the monomer degrees of freedom and treating the coils as soft colloids has great appeal. The review by Likos [88] provides an admirable survey of the soft colloid approach to polymers in solution.

Note that since $\phi(0) = \epsilon$ is finite particles can overlap. The homogeneous GCM has been investigated in great detail and the bulk structure and phase behaviour are well-studied [89, 90, 91]. In the (T, ρ) plane there is a region below $k_{\text{B}}T/\epsilon \approx 0.01$ where increasing ρ leads to freezing into a fcc phase, followed by a fcc-bcc transition, and then

melting so that the fluid is stable at high densities. For $k_B T/\epsilon > 0.01$ the fluid is stable at *all* densities. Detailed comparisons between the results of Monte Carlo simulations and integral equation theories of liquids have shown that for high densities the HNC approximation (5.16) provides an excellent account of the radial distribution function $g(r)$, the liquid structure factor $S(k)$ and the equation of state of the bulk fluid [90, 91]. It is argued [90] that the HNC should be exact in the limit $\rho R^3 \rightarrow \infty$. It is also observed that the very simple random phase approximation (RPA)

$$c^{(2)}(r) = -\beta\phi(r), \quad \forall r, \quad (5.50)$$

becomes accurate for very high densities $\rho R^3 > 5$ [90, 91]. This implies that the GCM behaves as a mean-field fluid over a very wide range of density and temperature. As the density increases the correlation hole becomes weaker and $g(r) \rightarrow 1$, for all separations r of the particles. Such behaviour is very different from that of fluids with hard cores where short-ranged correlations, induced by packing of the particles, always exist and become more pronounced at high density. For the soft-core GCM in the limit $\rho R^3 \rightarrow \infty$, the mean inter-particle separation $\rho^{-1/3}$ become much smaller than R so that a central particle interacts with a very large number of neighbours- a classic mean-field situation. Similar considerations apply to other positive definite, bounded pair potentials for which the RPA should also be valid at high density [90]. Note that (5.50) differs completely from (5.48). In the latter the RPA is applied to only the attractive tail of the pair potential; short-ranged correlations are included in the density dependent hard-sphere term. By contrast (5.50) applies to the *full* (repulsive) pair potential and the pair direct correlation function is independent of density ρ .

The simple mean-field (RPA) free energy functional that generates (5.50) is

$$\mathcal{F}_{\text{ex}}^{\text{RPA}} = \frac{1}{2} \sum_{i,j} \int d\mathbf{r} \int d\mathbf{r}' \rho_i(\mathbf{r}) \rho_j(\mathbf{r}') \phi_{ij}(\mathbf{r} - \mathbf{r}'), \quad (5.51)$$

where we have generalized to mixtures with pair potentials $\phi_{ij}(r)$. It is easy to check that $c_{ij}^{(2)}(r) = -\beta\phi_{ij}(r)$ follows from (5.51). In Ref. [91] it was shown that the one-component version of the functional (5.51) provides an accurate account of the density profiles of the GCM model adsorbed at a hard wall; results agree closely with those from Monte Carlo simulations.

Much attention has been focused on the properties of binary mixtures of repulsive Gaussian core particles since, for certain choices of mixing rules, these can exhibit fluid-fluid phase separation at sufficiently high total densities [91, 92]. Specifically a model

$$\phi_{ij}(r) = \epsilon_{ij} \exp(-r^2/R_{ij}^2), \quad (5.52)$$

with $i, j = 1, 2$, $\epsilon_{11} = \epsilon_{22} > \epsilon_{12}$ and $R_{12}^2 = (R_{11}^2 + R_{22}^2)/2$ exhibits demixing, driven by the positive nonadditivity as $R_{12} > (R_{11} + R_{22})/2$. In the (ρ, x) plane, where $\rho = \rho_1 + \rho_2$ is the total bulk density and x is the concentration of species 2, the mixture exhibits a binodal i.e. coexistence between a fluid phase rich in species 1 and one rich in species 2, at large values of ρ . The fluid-fluid coexistence curve ends at a lower consolute

point. Within the mean-field (RPA) treatment temperature scales out of the bulk free energy and the phase behaviour is that of an athermal system. Archer and Evans [92] investigated the interfacial density profiles and surface tension of the planar interface between demixed fluid phases of the binary mixture using the RPA functional (5.51). For certain coexisting states they found oscillations in the density profiles on both sides of the interface, i.e. approaching both bulk phases. In a subsequent study [93] the same authors investigated the wetting behaviour of the binary GCM at various, purely repulsive, planar walls. By following paths at fixed ρ , pre-wetting and complete wetting by the phase rich in species 1 were observed by decreasing the concentration x of species 2 towards coexistence.

The RPA functional (5.51) was also employed in studies of inhomogeneous binary star-polymer solutions [94]. Star polymers consist of a number of polymer chains, referred to as arms, covalently bonded to one common central core [88]. The arm number f , also termed the functionality, is the property that allows one to interpolate between linear chains ($f = 1, 2$) and the so-called colloidal limit $f \gg 1$ in which the stars resemble hard spheres. Unlike the GCM the effective potential [88] between the centres of two identical star polymers in an athermal solvent features a weak- $\ln(r/\sigma)$ divergence for separations $r \rightarrow \sigma$. For $r > \sigma$ and $f < 10$ the potential decays as a Gaussian. σ is the corona diameter. It is known that for one-component star polymers the HNC results are almost indistinguishable from those of simulation [88]. In Ref. [94] it was shown that for a binary mixture with $f = 2$, an additive mixture rule for the corona diameters: $\sigma_{12} = (\sigma_{11} + \sigma_{22})/2$ and a non-additive mixing rule for the ranges R_{ij} of the Gaussian tails similar to that employed in the binary GCM, the RPA generates a fluid-fluid binodal which is very close to that obtained from the much more sophisticated HNC. The RPA critical density is only slightly lower than that from HNC. Moreover the total pressure calculated at a fixed concentration $x = 0.5$ is extremely close to that from the HNC. The RPA also yields partial structure factors $S_{ij}(k)$ and radial distribution functions $g_{ij}(r)$ that are very close to their HNC counterparts at high total densities. For the planar free fluid-fluid interface the interfacial density profiles obtained from the functional (5.51) are very similar to those obtained for the binary GCM [94]. For a purely repulsive planar wall potential, with a soft logarithmically diverging core and a rapidly decaying (faster than Gaussian) tail designed to mimic star polymers at a hard wall, complete wetting with an accompanying pre-wetting transition was found-similar behaviour to that found in the GCM. By choosing $f = 2$ the star polymer pair potential corresponds to that between central monomers on a pair of polymer chains. This is a different perspective from the GCM: ‘central monomer’ versus ‘centre of mass’. However, since the same underlying polymer system should be described by both perspectives it is pleasing that these do lead to very similar bulk phase diagrams and interfacial phenomena [94].

One of the key advantages of employing the RPA functional (5.51) lies in its simplicity. For problems with planar [92] or spherical symmetry [95] the Euler-Lagrange equations resulting from minimizing the grand potential functional can be solved easily and very accurately using Picard iteration [51] even for sophisticated functionals. However, when the physical problems have less symmetry, so that the density profiles are

no longer dependent on a single variable z or r , it is most advantageous in numerical work if the Euler-Lagrange equations have a simple structure so some of the integrals can be performed analytically. An example is provided in Ref. [96] where the solvent mediated (SM) potential is calculated between two big colloidal particles immersed in a bulk binary mixture of smaller Gaussian core particles. Now the density profiles of the two solvent species have cylindrical symmetry and depend upon coordinates z (passing through the centre of the two colloids) and r (the radial distance from the z axis). Depending on how close the state point of the solvent is to the bulk binodal and the nature of the colloid-solvent interactions, thick ‘wetting’ films can develop around the colloids and bridging transitions can occur whereby two adsorbed films connect abruptly to form a single fluid bridge of the wetting phase. It would be much more difficult to investigate these subtle phenomena, with similar precision, using very sophisticated DFTs such as FMT for hard-core models. The formation of bridges has a profound effect on the SM potential making this very attractive.

Another simple model of a binary mixture that has been treated by the RPA functional (5.51) is that of purely repulsive point Yukawa pair potentials:

$$\phi_{ij}(r) = \frac{\epsilon M_{ij} \exp(-\lambda r)}{4\pi \lambda r}, \quad (5.53)$$

where the parameter $\epsilon > 0$ sets the energy scale, M_{ij} is the magnitude of the interaction between species i and j and λ is a common inverse length scale. Provided $M_{12} > \sqrt{M_{11}M_{22}}$ and the total density ρ is sufficiently high the mixture separates into two fluid phases—at least within the RPA [97]. The potentials (5.53) constitute a crude model for a binary mixture of charged colloidal particles in a charge-compensating solvent, i.e. λ is equivalent to the inverse Debye length κ . Classical Derjaguin Landau Verwey Overbeek (DLVO) theory [22] would imply $M_{12} = \sqrt{M_{11}M_{22}}$, since the amplitudes M_{ij} are proportional to the product of the charges $Z_i Z_j$ on the colloids. However, charge screening effects in the double layer of condensed counter ions can lead to a renormalization of the charges on the colloids and lead to deviations from this ideal Berthelot mixing rule and which might give rise to positive non-additivity so that the effective potentials between the colloidal particles satisfy $M_{12} > \sqrt{M_{11}M_{22}}$ [98].

In Ref. [97] it was shown that the radial distribution functions $g_{ij}(r)$ of the bulk fluid at states close to coexistence are well described by the RPA. Subsequently, using (5.51), it was shown that the binary Yukawa fluid wets completely a hard-wall and exhibits a pre-wetting transition slightly away from bulk coexistence [99]. In a later study [100] Hopkins et. al. calculated the SM potentials between model colloids or nanoparticles immersed in the binary solvent described by (5.53) using the functional (5.51) with the colloids treated as fixed particles exerting an external potential on the solvent. As in the case of the binary GCM, bridging transitions were found to occur for thermodynamic states sufficiently close to bulk coexistence. Bridging was also found to occur when a single large colloidal particle was brought close to a planar wall with an adsorbed wetting film [100]. The DFT approach was also used to investigate the interaction between a colloidal particle and the planar fluid-fluid interface [100]. All

three problems have density profiles with cylindrical symmetry: $\rho_i(z, r)$, which makes the numerics tractable.

We do not wish the reader to leave with the impression that the approximate functional (5.51) is a panacea for inhomogeneous soft-core fluids. This is certainly not the case since the RPA is valid only at high total densities where the mean-field description is a reliable approximation. The main advantage of employing (5.51) with simple model pair potentials is that it is fairly straightforward to implement numerically for situations where bulk phase separation occurs so that the subtle interfacial and adsorption *phenomena* that take place close to coexistence can be investigated with appropriate precision. Such phenomena play an important part in the fundamental physics and chemistry of solvation and in determining the effective interactions between big particles in a solvent that is close to phase separation (e.g. bridging), or to solvent criticality where the long-ranged correlations of the solvent have a profound influence on the effective interactions; this is the regime of critical Casimir forces. Of course, the mean-field description that is encompassed in (5.51), as with (5.45) for the LJ fluid, does not incorporate true criticality; the correlation length of the bulk fluid mixture decays with the classical exponent $1/2$ rather than the true value $\nu = 0.63$. This means that fluctuation effects are not incorporated properly in the DFT. Nevertheless, most of the physical phenomena that might occur in a proper treatment of criticality should be manifest in the RPA treatment.

Chapter 6

Concluding Remarks

In these lectures we have given a brief introduction to the formalism of equilibrium DFT and an overview of some progress in constructing approximate free energy functionals for three broad classes of fluids described by simple pair potentials.

For additive hard-sphere mixtures, Rosenfeld's FMT and its subsequent extensions and modifications have proved enormously successful when applied to a variety of inhomogeneous situations. Moreover, FMT provides an elegant geometric framework, based on deconvolution of the Mayer f -function, that gives much new insight into the nature of correlations and thermodynamic properties of uniform hard-particle fluids. The extensions of FMT to non-additive models, introduced by Schmidt and co-workers, have also been remarkably successful in applications to interfacial and adsorption problems as well as in describing the properties of the bulk mixtures. This is an area where we can expect to see many further developments. One outstanding problem for the DFT of additive hard-sphere mixtures is the case of large size asymmetry, i.e. when the size ratio q defined in Section 5.3.1 is very small. It remains to develop an accurate DFT approximation for such mixtures; these are important models for mixtures of colloidal particles. Non-spherical hard-particles bring their own challenges but the recent development of FMT in Ref. [79] is likely to spawn much activity and new understanding for systems where orientational ordering occurs.

For atomic fluids, where a Lennard-Jones type pair potential is a reasonable model, the functional (5.45) continues to be the most widely used-in spite of the shortcomings laid out in Section 5.3.2. Treating accurately a) soft repulsion and b) the attractive part of the potential present challenges. However, the approaches in Ref. [85] and [86] are steps forward.

For the third class of fluid, described by soft core repulsive potentials such as the GCM, the simple RPA or its mixture generalization provides a reasonably accurate description of the structure and thermodynamics of the bulk fluid at sufficiently high densities. This observation led to the adoption of the mean-field (RPA) functional (5.51) as an approximation for inhomogeneous soft core models. The simplicity of (5.51) and of the resulting Euler-Lagrange equations for the density profiles ensure that it is feasible to perform accurate numerical calculations for the profiles, determined by

the external potential $V(\mathbf{r})$, that do not have one-dimensional symmetry. This means that it is possible to investigate fluid structure and possible phase transitions, such as the formation of liquid bridges, in great detail for more complex confining geometries, thereby revealing the essence of the physical phenomena.

Acknowledgements

I am grateful to Pedro Tarazona for sending Ref. [50] and to Roland Roth for a preprint of Ref [51]. Both reviews go further into the theories and the applications of FMT than I can do here. Collaborations on DFT with Joe Brader, Roland Roth, Christos Likos, Matthias Schmidt, Andrew Archer, Jim Henderson, Maria Stewart, Martin Oettel and Paul Hopkins over the last ten years have been both enjoyable and rewarding. Yasha Rosenfeld, who introduced FMT in 1989, inspired and educated all of us working on DFT. Finally I wish to thank Harmut Löwen for helpful suggestions on the contents of our lectures, Brams Dwandaru for typing my notes and the School Organizers for their patience while I wrote these.

References

- [1] J.-P. HANSEN and I. R. McDONALD, *Theory of Simple Liquids*, Academic Press, 3rd Edition, 2006.
- [2] M. PLISCHKE and B. BERGERSEN, *Equilibrium Statistical Physics*, World Scientific, 3rd edition, 2006.
- [3] M. P. ALLEN and D. J. TILDESLEY, *Computer Simulation of Liquids*, Oxford University Press, 1987.
- [4] D. FRENKEL and B. SMIT, *Understanding Molecular Simulation From Algorithms to Applications*, Academic Press, 2002.
- [5] R. EVANS, in *Fundamentals of Inhomogeneous Fluids*, ed. D. Henderson, p. 85, Dekker, 1992.
- [6] N. D. MERMIN, *Phys. Rev.* **137**, A1441 (1965).
- [7] R. EVANS, *Adv. Phys.* **28**, 143 (1979).
- [8] J. T. CHAYES, L. CHAYES, and E. H. LIEB, *Commun. Math. Phys.* **93**, 57 (1984).
- [9] J. T. CHAYES and L. CHAYES, *J. Stat. Phys.* **36**, 471 (1984).
- [10] W. KOHN and L. J. SHAM, *Phys. Rev.* **140**, A1133 (1965).
- [11] J. R. HENDERSON, in *Fundamentals of Inhomogeneous Fluids*, ed. D. Henderson, p. 23, Dekker, 1992.
- [12] D. J. AMIT, *Field Theory: The Renormalisation Group and Critical Phenomena*, McGraw-Hill, 1978.
- [13] W. F. SAAM and C. EBNER, *Phys. Rev. A* **15**, 2566 (1977).
- [14] J. K. PERCUS, *J. Stat. Phys.* **15**, 505 (1976).
- [15] A. ROBLEDO, *J. Chem. Phys.* **72**, 1701 (1980).
- [16] A. ROBLEDO and C. VAREA, *J. Stat. Phys.* **26**, 513 (1981).

- [17] J. K. PERCUS, *J. Stat. Phys.* **28**, 67 (1982).
- [18] A. ROBLEDO and J. S. ROWLINSON, *Mol. Phys.* **58**, 711 (1986).
- [19] T. K. VANDERLICK, H. T. DAVIS, and J. K. PERCUS, *J. Chem. Phys.* **91**, 7136 (1989).
- [20] Y. ROSENFELD, *Phys. Rev. Lett.* **63**, 980 (1989).
- [21] S. FISK and B. WIDOM, *J. Chem. Phys.* **50**, 3219 (1969).
- [22] J.-L. BARRAT and J.-P. HANSEN, *Basic Concepts for Simple and Complex Liquids, Ch. 7*, Cambridge University Press, 2003.
- [23] J. E. ENDERBY, T. GASKELL, and N. H. MARCH, *Proc. Phys. Soc.* **85**, 217 (1965).
- [24] R. EVANS and J. R. HENDERSON, *J. Phys. Condens. Matter* **21**, 474220 (2009), and references therein.
- [25] J. A. BARKER and J. R. HENDERSON, *J. Chem. Phys.* **76**, 6303 (1982).
- [26] R. EVANS and T. J. SLUCKIN, *Mol. Phys.* **40**, 413 (1980).
- [27] J. S. ROWLINSON and B. WIDOM, *Molecular Theory of Capillarity*, Oxford University Press, 1982.
- [28] J. W. CAHN, *J. Chem. Phys.* **66**, 3667 (1977).
- [29] R. EVANS, in *Les Houches Session XL VIII: Liquids At Interfaces*, eds. J. Charvolin, J. F. Joanny and J. Zinn-Justin, p. 1, Elsevier, 1990.
- [30] R. EVANS, P. TARAZONA, and U. M. B. MARCONI, *Mol. Phys.* **50**, 993 (1983).
- [31] R. EVANS and U. M. B. MARCONI, *Phys. Rev. A* **34**, 3504 (1986).
- [32] J. R. HENDERSON, *Mol. Phys.* **52**, 1467 (1984).
- [33] T. V. RAMAKRISHNAN and M. YUSSOUFF, *Sol. St. Comm.* **21**, 389 (1977).
- [34] T. V. RAMAKRISHNAN and M. YUSSOUFF, *Phys. Rev. B* **19**, 2775 (1979).
- [35] A. D. J. HAYMET and D. W. OXTOBY, *J. Chem. Phys.* **74**, 2559 (1981).
- [36] J. K. PERCUS, in *The Equilibrium Theory of Classical Fluids*, eds. H. L. Frisch and J. L. Lebowitz, p. II 33, W. A. Benjamin, New York, 1964.
- [37] C. CACCAMO, *Phys. Rept.* **274**, 1 (1996).
- [38] J. L. BARRAT, J.-P. HANSEN, and G. PASTORE, *Mol. Phys.* **63**, 747 (1988).

- [39] M. DIJKSTRA, R. VAN ROIJ, and R. EVANS, *Phys. Rev. E* **59**, 5744 (1999).
- [40] M. DIJKSTRA, *Phys. Rev. E* **58**, 7523 (1998).
- [41] S. ASAKURA and F. OOSAWA, *J. Chem. Phys.* **22**, 1255 (1954).
- [42] S. ASAKURA and F. OOSAWA, *J. Polym. Sci.* **33**, 183 (1958).
- [43] A. VRIJ, *Pure Appl. Chem.* **48**, 471 (1976).
- [44] M. DIJKSTRA, J. M. BRADER, and R. EVANS, *J. Phys. Condens. Matter* **11**, 10079 (1999).
- [45] P. G. BOLHUIS, A. A. LOUIS, and J.-P. HANSEN, *Phys. Rev. Lett.* **89**, 128302 (2002).
- [46] H. REISS, H. FRISCH, and J. L. LEBOWITZ, *J. Chem. Phys.* **31**, 369 (1959).
- [47] E. KIERLIK and M. L. ROSINBERG, *Phys. Rev. A* **42**, 3382 (1990).
- [48] S. PHAN, E. KIERLIK, M. L. ROSINBERG, B. BILDSTEIN, and G. KAHL, *Phys. Rev. E* **48**, 618 (1993).
- [49] Y. ROSENFELD, D. LEVESQUE, and J.-J. WEIS, *J. Chem. Phys.* **92**, 6818 (1990).
- [50] P. TARAZONA, J. A. CUESTA, and Y. MARTINEZ-RATÓN, in *Density Functional Theories of Hard Particle Systems, Lect. Notes. Phys.*, **753**, p. 247, Springer, 2008.
- [51] R. ROTH, *J. Phys. Condens. Matter* (to appear).
- [52] Y. ROSENFELD, M. SCHMIDT, H. LÖWEN, and P. TARAZONA, *J. Phys. Condens. Matter* **8**, 1577 (1996).
- [53] P. TARAZONA, U. M. B. MARCONI, and R. EVANS, *Mol. Phys.* **60**, 573 (1987).
- [54] P. TARAZONA and Y. ROSENFELD, *Phys. Rev. E* **55**, R4873 (1997).
- [55] A. GONZALEZ, J. A. WHITE, F. L. RÓMAN, and R. EVANS, *J. Chem. Phys.* **109**, 3637 (1998).
- [56] P. TARAZONA, *Phys. Rev. Lett.* **84**, 694 (2000).
- [57] J. A. CUESTA, Y. MARTINEZ-RATÓN, and P. TARAZONA, *J. Phys. Condens. Matter* **14**, 11965 (2002).
- [58] P. TARAZONA, *Physica A* **306**, 243 (2002).
- [59] R. ROTH, R. EVANS, A. LANG, and G. KAHL, *J. Phys. Condens. Matter* **14**, 12063 (2002).

- [60] Y.-X. and J. WU, *J. Chem. Phys.* **117**, 10156 (2002).
- [61] Y.-X. YU, J. WU, Y.-X. XIN, and G.-H. GAO, *J. Chem. Phys.* **121**, 1535 (2004).
- [62] I. PAGONABARRAGA, M. E. CATES, and G. J. ACKLAND, *Phys. Rev. Lett.* **94**, 911 (2000).
- [63] D. GOULDING, S. MELCHIONNA, and J.-P. HANSEN, *Phys. Chem. Chem. Phys.* **3**, 1644 (2001).
- [64] H. HANSEN-GOOS and R. ROTH, *J. Chem. Phys.* **124**, 154506 (2006).
- [65] H. HANSEN-GOOS and R. ROTH, *J. Phys. Condens. Matter* **18**, 8413 (2006).
- [66] M. SCHMIDT, *J. Phys. Condens. Matter* **15**, S101 (2003).
- [67] J. M. BRADER, R. EVANS, and M. SCHMIDT, *Mol. Phys.* **101**, 3349 (2003).
- [68] M. SCHMIDT, H. LÖWEN, J. M. BRADER, and R. EVANS, *Phys. Rev. Lett.* **85**, 1934 (2000).
- [69] M. SCHMIDT, H. LÖWEN, J. M. BRADER, and R. EVANS, *J. Phys. Condens. Matter* **14**, 9353 (2002).
- [70] H. N. W. LEKKERKERKER, W. C. K. POON, P. N. PUSEY, A. STROOBANTS, and P. B. WARREN, *Europhys. Lett.* **20**, 559 (1992).
- [71] M. SCHMIDT, A. R. DENTON, and J. M. BRADER, *J. Chem. Phys.* **118**, 1541 (2003).
- [72] M. DIJKSTRA and R. VAN ROIJ, *Phys. Rev. Lett.* **89**, 208303 (2002).
- [73] M. SCHMIDT, A. FORTINI, and M. DIJKSTRA, *J. Phys. Condens. Matter* **15**, S3411 (2003).
- [74] I. O. GÖTZE, J. M. BRADER, M. SCHMIDT, and H. LÖWEN, *Mol. Phys.* **101**, 1651 (2003).
- [75] M. SCHMIDT, M. DIJKSTRA, and J.-P. HANSEN, *Phys. Rev. Lett.* **93**, 088303 (2004).
- [76] B. WIDOM and J. H. ROWLINSON, *J. Chem. Phys.* **52**, 1670 (1970).
- [77] M. SCHMIDT, *Phys. Rev. E* **63**, 010101 (2000).
- [78] M. SCHMIDT, *J. Phys. Condens. Matter* **16**, L351 (2004).
- [79] H. HANSEN-GOOS and K. MECKE, *Phys. Rev. Lett.* **102**, 018302 (2009).
- [80] R. EVANS, J. R. HENDERSON, and R. ROTH, *J. Chem. Phys.* **121**, 12074 (2004).

- [81] M. C. STEWART and R. EVANS, *Phys. Rev. E* **71**, 011602 (2005).
- [82] M. C. STEWART and R. EVANS, *J. Phys. Condens. Matter* **17**, S3499 (2005).
- [83] R. LIPOWSKY, *Phys. Rev. B* **32**, 1731 (1985).
- [84] T. WADEWITZ and J. WINKELMANN, *J. Chem. Phys.* **113**, 2447 (2000).
- [85] J. F. LUTSKO, *J. Chem. Phys.* **128**, 184711 (2008).
- [86] M. OETTEL, *J. Phys. Condens. Matter* **17**, 429 (2005).
- [87] P. G. BOLHUIS, A. A. LOUIS, J.-P. HANSEN, and E. J. MEIJER, *J. Chem. Phys.* **114**, 4296 (2001).
- [88] C. N. LIKOS, *Phys. Rep.* **348**, 267 (2001).
- [89] F. H. STILLINGER and D. K. STILLINGER, *Physica A* **244**, 358 (1997).
- [90] C. N. LIKOS, A. LANG, M. WATZLAWEK, and H. LÖWEN, *Phys. Rev. E* **63**, 031206 (2001).
- [91] A. A. LOUIS, P. G. BOLHUIS, and J.-P. HANSEN, *Phys. Rev. E* **62**, 7961 (2000).
- [92] A. J. ARCHER and R. EVANS, *Phys. Rev. E* **64**, 041501 (2001).
- [93] A. J. ARCHER and R. EVANS, *J. Phys. Condens. Matter* **14**, 1131 (2002).
- [94] A. J. ARCHER, C. N. LIKOS, and R. EVANS, *J. Phys. Condens. Matter* **14**, 12031 (2002).
- [95] A. J. ARCHER and R. EVANS, *J. Chem. Phys.* **118**, 9726 (2003).
- [96] A. J. ARCHER, R. EVANS., R. ROTH, and M. OETTEL, *J. Chem. Phys.* **122**, 084513 (2005).
- [97] P. HOPKINS, A. J. ARCHER, and R. EVANS, *J. Chem. Phys.* **124**, 054503 (2006).
- [98] E. ALLAHYAROV and H. LÖWEN, *J. Phys. Condens. Matter* **21**, 424117 (2009).
- [99] P. HOPKINS, A. J. ARCHER, and R. EVANS, *J. Chem. Phys.* **129**, 214709 (2008).
- [100] P. HOPKINS, A. J. ARCHER, and R. EVANS, *J. Chem. Phys.* **131**, 088303 (2009).